Polymer Chemistry

ROYAL SOCIETY OF CHEMISTRY

MINIREVIEW

View Article Online
View Journal | View Issue

Cite this: *Polym. Chem.*, 2021, **12**, 5724

Evolution and applications of polymer brush hypersurface photolithography

Daniel J. Valles,[a,b,c] Yerzhan S. Zholdassov[a,b,c] and Adam B. Braunschweig *[a,b,c,d]

Hypersurface photolithography (HP) is a printing method for fabricating structures and patterns composed of soft materials bound to solid surfaces and with ~1 micrometer resolution in the *x*, *y*, and *z* dimensions. This platform leverages benign, low intensity light to perform photochemical surface reactions with spatial and temporal control of irradiation, and, as a result, is particularly useful for patterning delicate organic and biological material. In particular, surface-initiated controlled radical polymerizations can be leveraged to create arbitrary polymer and block-copolymer brush patterns. Here we will review advances in instrumentation architectures that have made these hypersurfaces possible, and the investigations and development of surface-based organic chemistry and grafted-from photopolymerizations that have arisen through these investigations. Over the course of this discussion, we describe specific applications that have benefited from HP. By combining organic chemistry with the instrumentation developed, HP has ushered in a new era of surface chemistry that will lead to new fundamental science and previously unimaginable technologies.

Received 10th August 2021,
Accepted 23rd September 2021

DOI: 10.1039/d1py01073e

rsc.li/polymers

Introduction

Polymer brushes[1–3] – polymer chains that are tethered to a surface – could be used to fabricate soft-matter structures possessing nanoscale dimensions and complex topographies and whose functions are comparable to complex biological interfaces.[4] For example, biologically active polymer brushes found on cell surfaces are involved in communication, digestion, pathogen invasion, or immune response. Mimicking cell-surface biopolymers can be used to increase the current under-

[a]*Advanced Science Research Center at the Graduate Center of the City University of New York, 85 St Nicholas Terrace, New York, NY 10031, USA.*
E-mail: abraunschweig@gc.cuny.edu
[b]*Department of Chemistry, Hunter College, 695 Park Ave, New York, NY 10065, USA*
[c]*PhD Program in Chemistry, Graduate Center of the City University of New York, 365 5th Ave, New York, NY 10016, USA*
[d]*PhD Program in Biochemistry, Graduate Center of the City University of New York, 365 5th Ave, New York, NY 10016, USA*

Daniel J. Valles

Daniel J. Valles received his B.S. in Chemistry from SUNY Stony Brook University and M.A. in Chemistry from CUNY Brooklyn College. He recently defended his thesis to complete his PhD in Chemistry at the CUNY Graduate Center under the guidance of Prof. Adam B. Braunschweig at the Advanced Science Research Center. Daniel's research has focused on developing lithography techniques for patterning organic, macromolecular, and biological materials.

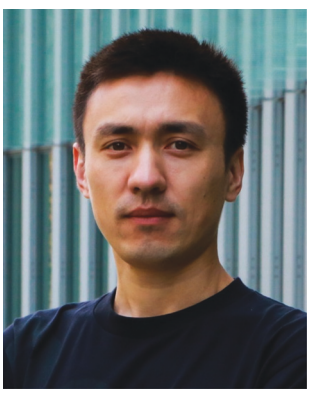

Yerzhan S. Zholdassov

Yerzhan S. Zholdassov obtained his B.Sc. in Chemical Technology from South Kazakhstan State University, Kazakhstan and M. Sc. in Chemical Technology from Gubkin Russian State University of Oil and Gas, Russian Federation under the supervision of Professor Vladimir M. Kapustin. He is currently working under the guidance of Professor Adam B. Braunschweig at the Advanced Science Research Center. Yerzhan's research focuses on polymer brush nanolithography and surface-initiated polymerization chemistries.

standing of the role of membrane-bound biopolymers in biological regulation and how the subtleties of their binding and response to stimuli contribute to their biological roles. Alternatively, surfaces patterned with polymer brushes could find applications as advanced materials, including in optics,[5] antifouling surfaces,[6] displays,[7] electronics,[8] and cryptography.[9] The envisioned advanced materials or synthetic mimics of these complex biological interfaces (Fig. 1) would be an arrangement of brushes spread across a surface segregated into thousands-to-millions of individual areas on the x, y plane of the substrate, which are referred to as pixels. In these structures the height and composition of the polymer brushes at each pixel of the surface could be individually varied, the diameter or edge length of each pixel across the surface should be <1 micrometer, and the height of each polymer brush pixel should be controllable to within <10 nm. One can even envision structures of these polymer brush patterns where composition along a chain could be controlled by printing block copolymer brushes. We refer to such structures as 'polymer brush hypersurfaces' and not '3D prints' or '3D structures' because the three cartesian dimensions are not sufficient to define their structure. For example, defining any voxel – a unit of volume in a three-dimensional structure[10] – in the block copolymer hypersurfaces would require at least 4 orthogonal dimensions – (i and ii) x, y position across the surface, (iii) height, z, and (iv) chemical composition. Rather than refer to these objects as '4D prints', '4D structures', or '4D surfaces', we use the term hypersurface[11] because '4D printing' has already been coopted by the printing community to refer to objects whose structures change with time,[12,13] and to also recognize that these polymer brush patterns may necessitate more than 4 variables for a complete description. So any method for printing polymer brush hypersurfaces would allow users to control patterning with compositional control at the single voxel level of resolution, and such a polymer brush hypersurfaces with sub-1 μm^3 voxel volume would have potential applications including in biosensors,[14–16] stimuli-responsive materials,[9,17,18] electronics,[19–23] for tissue engineering,[24] or in any field where complex, multidimensional polymer brush objects with micrometer or sub-1 μm^3 voxel resolution is required. In this review, we briefly describe printing techniques and immobilization strategies that have been utilized for creating topologically sophisticated synthetic soft matter surfaces, what challenges needed to be addressed to construct polymer brush hypersurfaces, and how our group furthered printing technology and surface chemistry to build complex polymer brush hypersurfaces.

Two major challenges have precluded the fabrication of these multidimensional polymer brush hypersurfaces, and, as a direct result, these objects have not been widely adopted by the research and industrial communities. The first challenge is inadequate printing instrumentation. A hypersurface printer must have the following attributes. It must be able to achieve pixels with ~1 micrometer-scale or sub-micrometer scale diameters or edge lengths. It must possess a means of controlling height independently at each pixel. It must offer a strategy for varying chemical composition at each pixel and along a polymer brush. Ideally these printers would also produce patterns that cover a large (>1 cm^2) area, do not require excessive print times, and are inexpensive. The second challenge, chemistries for growing the polymer brushes off the surface, are equally responsible for hindering the development of polymer brush hypersurface lithography. The selected chemistries must provide a polymer brush that is anchored to the surface, can control height precisely, provide a means to vary composition along a chain, and, importantly, must be a reaction that can be spatiotemporally controlled by the hypersurface printer, meaning that the printer can independently turn the reaction on or off at each pixel in the surface. Thus, the instrumentational and chemical requirements are very difficult to meet in a single printer, and, until hypersurface photolithography (HP) was first reported,[25] no printer had combined all of these capabilities into a single platform.

The most common microlithographic tools, which are those used for creating integrated circuits,[26] are inadequate for producing soft-material hypersurfaces,[27–29] and HP was made possible by building upon significant progress in alternative lithographic methods that were specifically developed for the micropatterning and nanopatterning of soft materials. Top-down microfabrication tools, such as electron-beam, ion beam, or extreme UV lithography, whittle away a solid structure using high energy irradiation that would denature or even destroy biological and organic materials.[29] In addition, even when strategies for creating polymer brush hypersurfaces could be devised using these lithographies, the specialized tools and facilities needed are prohibitively expensive and would exclude many researchers. Nevertheless, polymer brush patterns and even multiplexed polymer brush patterns have been created using conventional photolithography.[30–35] Generally, these structures are created by taking a substrate with initiators that are uniformly coated across the surface, immersing this substrate in a monomer solution, and using light passing through the reactions to grow the polymers *via* photochemical propagation reactions from the surface only where irradiation through a photomask is occurring. These reactions, where the polymers propagate from surface-bound

Adam B. Braunschweig

Prof. Adam B. Braunschweig joined the Nanoscience Initiative at the Advanced Science Research Center at the City University of New York and the Department of Chemistry at Hunter College in 2016. His group investigates nanolithography of soft matter, photophysics of supramolecular systems, synthetic carbohydrate receptors, and the structure and properties of natural and synthetic mucins.

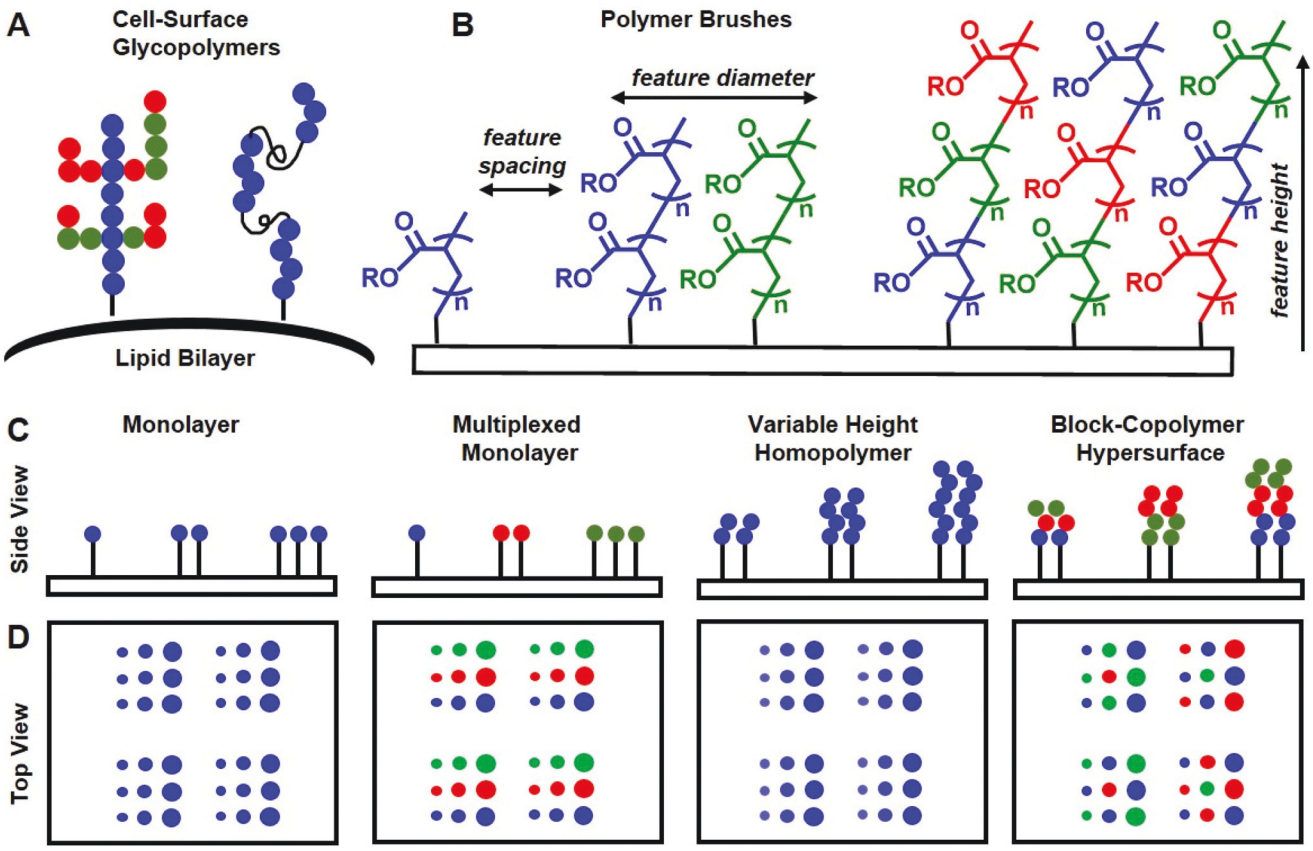

Fig. 1 (A) Cell surfaces are an example of a biological interface coated with biopolymer brushes, such as glycolipids and glycopolymers. (B) Different factors that must be considered in patterning polymer brushes include brush composition, feature height, feature diameter, and feature-to-feature spacing. (C) Side view of the different types of surfaces and patterns that can be made from brush polymers and brush copolymers using hypersurface photolithography. (D) A top-down view of the different types of surfaces and patterns that can be made from brush polymers and brush copolymers using hypersurface photolithography.

initiators, are referred to as 'grafted-from' polymerizations, and are preferable for making hypersurfaces over 'grafted-to' reactions, where pre-formed polymers are then deposited onto a surface.[3,36] For example, if one were to make a hypersurface with 1000 different polymers using a grafting-to approach, then one would have to run 1000 reactions in solution, purify the polymers, and then transfer them from solution to the surface, which often requires more material and time than can be reasonably dedicated to printing a single surface. However, grafted-from reactions can consume minute amounts of monomer, can be run in parallel, where different brushes are grown simultaneously at different pixels, require minimal post-polymerization purification, and eschew altogether post-polymerization immobilization to the substrate.

The Hawker group, for example, has extensively explored light-mediated atom transfer radical polymerization (ATRP) chemistry for grafting polymer brushes from surfaces. Upon activation of a photocatalyst by exposure to visible light, monomers propagate from the surface, and the polymerization can be halted by simply turning off the light.[37–40] With this chemistry, brush polymers were patterned by irradiating through a conventional photomask, where growth is spatially confined to light-exposed areas, leaving the unexposed regions with active initiators for subsequent polymer brush growth. This method was also used to generate polymer brush gradients by employing a neutral density filter to moderate the intensity of light hitting different regions of the surface, which, in turn, spatially moderated the rate of polymer brush propagation.[41] The same group patterned five different emissive polymers onto the same surface, where the dopant incorporation, position of brush growth, and brush thickness are controlled by exposing the surface with light through a series of photomasks or utilizing wavelength dependent photocatalysts, and these methods were used to fabricate organic light emitting diodes.[5] Photochemical polymerization on surfaces *via* photolithography was used by others for discovering new photocatalysts[42] and constructing oxygen tolerant polymerization systems[43] by employing surface-initiated ATRP and surface-initiated radical addition–fragmentation chain transfer polymerization, respectively. Several limitations of using successive photomasks to create multiplexed polymer brush patterns, however, continue to preclude the facile fabrication of complex, arbitrary, polymer brush hypersurfaces. These include the limitations that each new material that is patterned onto the

surface requires its own expensive photomask or elaborate photoinitiator schemes; polymer brushes of different lengths are not easily prepared with the same photomask; and the need to align each new photomask with the substrate limits resolution and, in turn, prevents the printing of block copolymer hypersurfaces, where the length of each block at each pixel can be independently controlled.

Alternatively, soft lithography methods such as microcontact printing (μCP)[44–48] and dip-pen nanolithography (DPN)[49–52] have been used to create grafted-from polymer brush patterns. μCP relies upon elastomeric stamps to pattern molecules onto substrates. Stamps for μCP are made by microfabricating a mold, also known as a master, of the desired pattern from a silicon wafer and then curing an elastomeric polymer in the mold. After peeling the polymer from the master, a liquid 'ink', composed of the materials that will be delivered to the surface, is deposited directly onto the stamp. The stamp is then pressed onto the surface, delivering the ink to the substrate to form patterns. Because μCP does not use destructive, high-energy irradiation, it is advantageous for patterning many types of soft materials including organic molecules,[53–55] DNA,[56–58] proteins,[59–61] lipids,[62,63] glycans,[64–66] and nanoparticles.[67–69] Polymer brush patterns can be created by μCP by using the elastomeric stamp to pattern an initiator onto a surface, and the polymer brushes are grown from the surface by immersing the substrate in a monomer solution and propagating the polymers thermally.[70] Demonstrated applications of the resulting prints include organic LEDs,[71] thin-film transistors,[72,73] integrated circuits,[74,75] and microoptical parts,[71,76] or for controlling cell adhesion.[77,78] Alternatively, DPN relies upon an atomic force microscope (AFM) tip that is coated with an ink and mounted onto the z-piezo actuator of an AFM. As the tip is repeatedly brought into contact with the surface, the ink travels through an aqueous meniscus formed between the tip and the surface to create a pixel composed of the ink deposited from the tip. By moving the tip with respect to the surface, a pattern is created with sub-micrometer control of feature diameter and feature-to-feature spacing (pitch).[79] DPN has been used to pattern small molecules,[80] metals[81–85] and insulators,[86] biopolymers such as DNA,[87,88] proteins,[89–92] antibodies,[93] peptides,[94–96] and nanomaterials.[97–99] Polymer brushes have been patterned with DPN by using the AFM tips to deposit an initiator onto a surface, and polymers are subsequently propagated thermally from the surface by immersing the substrate in an appropriate monomer solution.[100–104] Zheng *et al.*, for example, patterned initiators for ATRP by DPN and subsequently grew polymer brush features with sub-1 micrometer diameters and heights of ~35 nm.[105] Based on their study, they determined that the height and grafting density of the polymer were dependent on the force exerted onto the surface by the tip as well as the dwell time of the tip when depositing the initiator. Alternatively, Riedo *et al.* developed a technique called thermochemical nanolithography, in which an AFM tip is heated to site-specifically induce thermochemical reactions on a monomer-coated surface.[106,107] Both of these methods, μCP and DPN, are relatively low-cost, bottom-up strategies that are non-destructive, which makes them more attractive methods for patterning soft materials. Their drawbacks, however, preclude them from being general solutions to the challenge of preparing polymer brush hypersurfaces. In μCP, the stamps have a typical feature diameter that can only be reduced below ~1 μm with difficulty, and the distance between features is limited by capillary adhesion if they are too close together and roof collapse if they are too far apart, thereby imposing major constraints on the pattern design.[108,109] DPN offers more flexibility in terms of pattern design and can create features with diameters <100 nm, but patterning areas are small – typically ~100 μm^2. Finally, no realistic approaches have been developed to create multiplexed patterns with either μCP or DPN, where features of different materials can be patterned arbitrarily and with sub-1 micrometer control over the registration between features of different compositions.

So both conventional top-down microfabrication and bottom-up soft lithography methods have limitations that preclude them from providing general solutions to the polymer brush hypersurface challenge. Yet, of these methods, DPN, and, more generally, scanning probe lithographies (SPLs), which are nanolithography techniques that involve scanning probes to create patterns, have laid the foundation for modern hypersurface printers. Specifically, efforts in the Mirkin group[49] devoted to increasing printing area, developing new tip architectures and multiplexing strategies, and coupling alternate forms of energetic activation, laid the foundation necessary for the evolution of SPL into HP. One of the most important of these advances was the development of massively parallel elastomeric tip architectures.[49,110,111] Although silicon-based tip architectures with as many as 55 000 tips had been microfabricated,[112] these were difficult to prepare and hard to use. In 2008, Huo *et al.* described the first massively-parallel SPL, termed polymer pen lithography (PPL),[110] a major breakthrough in SPL in which the cantilever-based AFM tips used for DPN were replaced with elastomeric pyramids arranged into 2D grids with as many as 10^7 tips. Upon mounting polymer pen arrays coated with inks onto the piezoelectric actuators of an AFM, patterns were made in a similar fashion to DPN, in which ink transits from the tips through an aqueous meniscus and onto the substrate. The significance of PPL is that patterns could be made over large (>1 cm^2) areas, while still maintaining many of the advantages of DPN, including sub-1 micrometer pixel diameters, wide materials compatibility, and the ability to create patterns without necessitating a photomask. Since it was first reported, PPL has already been used to create patterns of biomolecules, such as DNA,[113,114] proteins,[115,116] lipids,[117,118] glycans,[119,120] small organic molecules,[110] polymers,[121–123] and nanomaterials.[124,125] Two drawbacks of PPL, however, preclude this method from providing a general solution to the problem of printing polymer brush hypersurfaces. These are that each pixel is composed of the same material, and every tip in the array produces the same pattern or image, and so a single pattern is repeated thousands of times across the surface. To address the former chal-

lenge, several strategies for creating multiplexed patterns have been attempted. For example, PPL multiplexing was accomplished by using[115,126] inkwells to load different inks onto a polymer pen array, but the pattern created by any pen in the PPL array contained only a single ink. Other strategies are based on depositing inks onto pads to dip the arrays into[116] or depositing the inks directly onto[114] the arrays *via* pipetting and spin coating of the inks. These approaches, however, place strict limitations on the patterns that can be printed, and the majority of the surface is sacrificial. So none of these strategies truly solve the multiplexing challenge in that a very limited number of different inks are patterned in the same array, and it is very difficult to create pixels of different inks in close proximity. As such, a major unaddressed challenge in SPL remained, namely the inability to create multiplexed patterns, where the chemical composition of any pixel in the pattern could be varied arbitrarily (Fig. 2).

Creating arbitrary patterns with each tip in the array was successfully solved by coupling advanced optics and microfluidics – initially with pen arrays and then eventually by removing them altogether. The term 'arbitrary pattern' is intended to mean that the image or pattern created by each pen in the array is different, leading to a single, coherent image coating the entire patterning area, rather than a smaller, less complex pattern being repeated by each pen across the array. The key advance to creating arbitrary patterns by SPL was the development of 'beam pen arrays', in which the massively parallel polymer pen arrays are coated with an opaque metal, except for an aperture at the tip that allows for the passage of light. So, beam pen lithography[127] (BPL) is when these arrays are mounted onto an AFM, the arrays are illuminated from the backside, and light traveling through the apertures induces a photochemical reaction. BPL has been used to investigate several photoinduced organic reactions and grafted-from polymerizations, including thiol–ene click reactions,[128,129] and controlled-radical polymerizations,[130] respectively, or for electronics fabrication by using the light that transits through the apertures to expose conventional photoresists.[127] Given that low-dose or low-energy irradiation can be delivered to a surface by BPL, while still achieving sub-diffraction feature diameters, it has been used to make nanopatterns of biomolecules, such as glycans[130] or DNA,[131] as well as small organic molecules[128,129] and polymers.[130] In the initial demonstrations of BPL, all tips produced the same patterns, but this problem was soon resolved by introducing a digital micromirror device (DMD) into the optical path between the light source and the tip arrays.[19] A DMD is a chip coated with hundreds-of-thousands of individually actuatable mirrors that, under the control of a CPU, can either direct light onto or away from individual tips in the underlying BPL array. And so a printer that includes a DMD and a beam pen array can control the spatiotemporal delivery of light to each individual tip in the BPL array to create arbitrary patterns whose minimum pixel diameters are determined by the width of the apertures in the metal coatings in the tip arrays. The capabilities of this new printer architecture, involving both BPL arrays and a DMD, were demonstrated by fabricating electronics,[19] and creating arbitrary patterns of small organic molecules,[132–135] and DNA.[136]

PPL, BPL, and other SPLs based on massively parallel tip arrays had addressed many of the challenges needed to print polymer brush hypersurfaces – soft-matter compatibility, printing arbitrary patterns over large areas, and achieving sub-1 micrometer feature diameters. Two important criteria needed for any hypersurface printer, however, remained unsolved. These were the ability to create truly multiplexed patterns, where there are no limitations on where each ink can be printed, and a method of controlling the height of each pixel in a polymer brush pattern. Here we describe the advances in both chemistry and instrumentation that have led to the recent emergence of true hypersurface printers that can make these arbitrary, multiplexed hypersurfaces from grafted-from polymer brushes. Finally, we give examples of how these printers are being used to address a pressing scientific questions, including creating more accurate models of biological interfaces to achieve a more nuanced understanding of biological recognition at interfaces or creating stimuli-responsive surfaces for cryptographic applications.

Discussion

Even with DMD-equipped BPL, there still remained a need for advances in both chemistry and instrumentation before polymer brush hypersurfaces could be realized. The major chemical challenge involved increasing the number of bond-forming reactions that could be used to modify solid-surfaces, validating accessible characterization methods for confirming

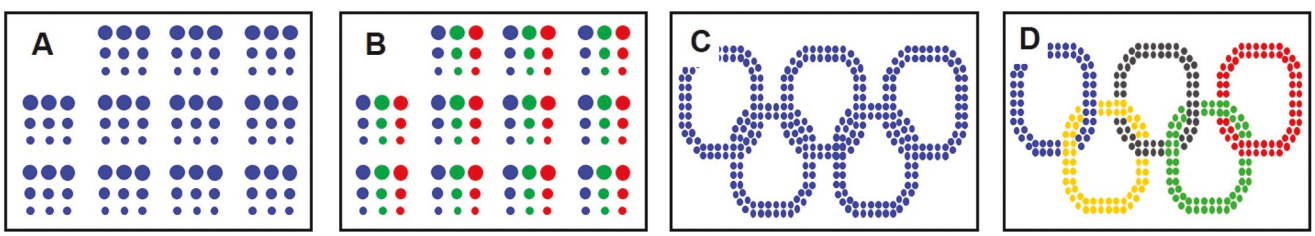

Fig. 2 (A) Single-ink pattern being repeated by each pen across the array. (B) Multiple-ink pattern being repeated by each pen across the array. (C) Arbitrary pattern created from a single ink. (D) Arbitrary pattern created with multiple inks.

bond formation, and increasing reaction throughput, so that tens or even hundreds of different reaction conditions could be tested in a reasonable timeframe. The latter is particularly important because researchers investigating and optimizing reactions in solution typically carry out many reactions before determining ideal conditions, and the low throughput of surface reactions – determined by the time for setting up and characterizing a reaction – has slowed significantly the development of surface chemistries, such that of the myriad organic reactions known, few have been used to alter the chemical composition of surfaces.[28] Characterization challenges arise because the analytical techniques that are used to characterize the products of reactions carried out in solution, such as nuclear magnetic resonance (NMR) spectroscopy or mass spectrometry (MS), are not easily adapted to characterize the composition of functionalized substrates, and, as such, new solutions to the characterization challenge must be devised.[137] To increase the numbers of reactions that can be used to modify the composition of a surface, SPL techniques have been used to immobilize molecules onto surfaces with metal catalyzed,[138] enzyme catalyzed,[139] thermal,[106] redox,[140] force,[141] and light-induced reactions.[9,14–16,25,128,130,142,143] Of these, the photochemical reactions are the most promising as light is a particularly easy activation source to spatiotemporally localize with appropriate optics. However, to construct hypersurfaces with any of these surface chemistries, there are still major challenges that need to be addressed such as reducing feature diameter, spatiotemporal control of chemistry in 3D, and construction of block-copolymers. Finally, a multiplexing strategy must be devised so that a different polymer brush could be immobilized at each pixel on the surface. As such, there was a need to further develop photochemical polymer propagation reactions and adapt them for and integrate them with the appropriate instrumentation. Such instrumentation did not exist, and what was needed was a new platform that could achieve the targeted feature dimensions, introduce different inks, and localize the stimulus that drives the polymer propagation. Herein, we highlight our work in advancing both surface chemistry and printing instrumentation, which have resulted in the first platform for creating polymer brush and block copolymer brush hypersurfaces. We summarize a selection of these reports from our group and, in doing so, show how each was a step towards the larger goal of creating the necessary instrumentation and chemistry to prepare polymer brush hypersurfaces with structural complexity and functionality comparable to biological interfaces.

Spatially controlled covalent bond formation over 1 cm^2 areas

The first challenge that we sought to address was to show that patterns could be created by using massively parallel polymer pen arrays to induce spatially localized covalent bond formation. By doing so, we would demonstrate this important proof-of-concept, while simultaneously learning to address the major challenges involved with inducing organic reactions on surfaces and characterizing the products of these transformations. The difficulty associated with characterizing the products of covalent reactions on surfaces arises because the formation of new bonds cannot be determined using the conventional spectroscopic methods applied to reactions carried out in solution, such as NMR and MS. In addition, the instrumentation that can directly detect the formation of new covalent bonds on surfaces, such as X-ray photoelectron spectroscopy (XPS) or Raman mapping, are low-throughput, expensive, and not widely available. Thus, finding appropriate characterization methods that are accessible and higher throughput are important because optimizing organic surface reactions potentially requires hundreds of experiments, and so rapid quantitative analysis is essential for having a tractable reaction optimization timeline. An alternative to relying upon expensive and rare instrumentation is to design inks that are detectable on common, inexpensive, and high-throughput equipment. To this end, we have found redox-active and fluorescent inks to be particularly useful because their immobilization can be monitored by broadly accessible electrochemical, fluorescent, and AFM methods.

In this report, we used "click" chemistry to create new bonds between functionalized surfaces and molecules within the inks (Fig. 3A). The molecules were designed to facilitate characterization, and PPL was used to pattern the ink onto the surface. Click reactions[144] are biorthogonal surface chemistries that generally have high yields, minimal byproducts, and, as a

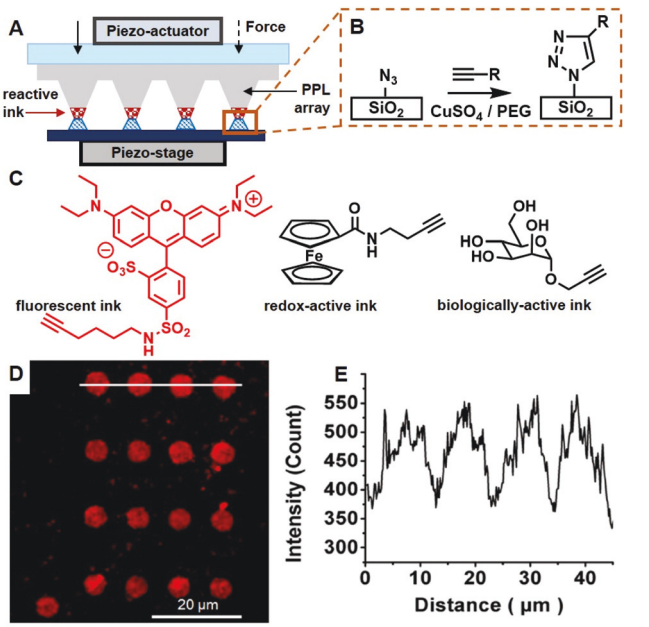

Fig. 3 (A) Polymer pen lithography uses elastomeric tips to transfer molecules onto a surface *via* an aqueous meniscus. (B) Cu^{I}-Catalyzed azide–alkyne click chemistry used to immobilize different alkyne-labeled inks onto an azide functionalized surface. (C) Three inks that were prepared and printed to facilitate characterization by fluorescence microscopy or electrochemistry, or to assess binding to fluorescently-labelled glycan-binding proteins (GBPs). (D) Fluorescence microscopy image of patterned alkyne-labelled mannose after exposure to a solution of fluorescently-labelled ConA, a mannose-specific GBP, which confirmed bioactivity. (E) Intensity profile of the white line in (D).

result, are ideal chemistries to pattern organic and bioactive molecules and validate the instrumentation as a platform for surface organic chemistry. The Cu^{I}-catalyzed azide–alkyne cycloaddition (CuAAC) click reaction was used to induce the formation of a new triazole linkage on a surface by reacting alkyne-labeled reagents transferred by the tip onto a surface functionalized with terminal azide groups (Fig. 3B).[119] Two different inks (Fig. 3C), alkyne-labelled rhodamine and alkyne-labelled ferrocene, were prepared because their immobilization could be detected by fluorescence microscopy and cyclic voltammetry (CV), respectively, which are both widely accessible and relatively affordable characterization tools. A third ink, α-D-mannose, that can bind to the mannose-specific glycan binding protein (GBP) concanavalin A (ConA), was synthesized to confirm that the deposited molecules maintained their native biological activity. These molecules were immobilized by coating them onto a polymer pen array in a mixture with the Cu-catalyst, a reducing agent, and polyethylene glycol, which is added as an agent to facilitate uniform transfer from the tip to the surface by encapsulating all materials and thereby ensuring that all materials necessary for the complex reaction to proceed are delivered to the surface in the appropriate ratios.[123] Arrays of rhodamine-alkyne were successfully transferred to the surface by PPL, and, upon washing, patterns with sub-1 μm features over large areas (>1 cm^2) were visible by fluorescence microscopy (Fig. 3D). The surface coverage density was determined by CV of a surface reacted with the ferrocene ink. Finally, the ability of the patterned features to maintain biological activity was demonstrated by covalently patterning α-D-mannose and exposing the surface to a solution of fluorescently-labelled ConA. The fluorescent features indicated that the immobilized glycan was indeed recognized by ConA, although fluorescence signal was relatively low (Fig. 3E). This study established that PPL combined with organic chemistry can be used to pattern and covalently immobilize organic molecules onto solid interfaces without relying on expensive instrumentation, thereby lowering the barrier to surface-reaction discovery. To demonstrate the generalizability and ease with which PPL can be used to induce and study thermally activated organic transformations on surfaces, fluorescent patterns were prepared by delivering aryl phosphine-labelled fluorophores, which reacted with an azide-labelled surface *via* a Staudinger ligation.[145] While these reports addressed important challenges for performing organic chemistry on surfaces, several requirements for achieving HP remained unaddressed, including the ability to multiplex – in the above work, each print explored only a single set of reaction conditions, thereby slowing reaction optimization. Additionally, the reactions demonstrated were not polymerizations, thereby limiting patterning to two dimensions.

Spatially controlled photochemical 3D nanolithography

The next challenge we sought to address was using spatially controlled photochemistry to induce surface reactions for fabricating polymer brush arrays. To do so, BPL arrays were used to deposit organic molecules onto appropriately functionalized surfaces, and the features were subsequently irradiated through the beam pen array to photochemically initiate covalent bond formation. Photoinduced thiol–ene click reactions[146–148] were selected as the first candidates for attempting to form covalent bonds photochemically because these reactions proceed in high yield, bonds form rapidly, and the reaction is biorthogonal.[147] BPL arrays were used to localize the catalytic irradiation to form the pixels in the resulting pattern (Fig. 4A). We studied both the thiol–ene click reaction (Fig. 4B) between inks functionalized with thiols with an alkene-terminated surface, and, alternatively the thiol–acrylate reaction between acrylate-functionalized inks with thiol-functionalized surfaces. We confirmed photochemical bond-formation, and studied reaction kinetics by varying the irradiation times for different features in the same print, and, in doing so, made the surprising discovery that led to the advent of nanoscale 3D printing.

In this work, light was focused through beam pen arrays onto small areas of the surface that had already been patterned with the reactive inks. Kinetic studies of the reactions between printed dyes (Fig. 4C) and the complementary surfaces were performed by varying the exposure time of light onto each feature in a pattern, and the resulting features were

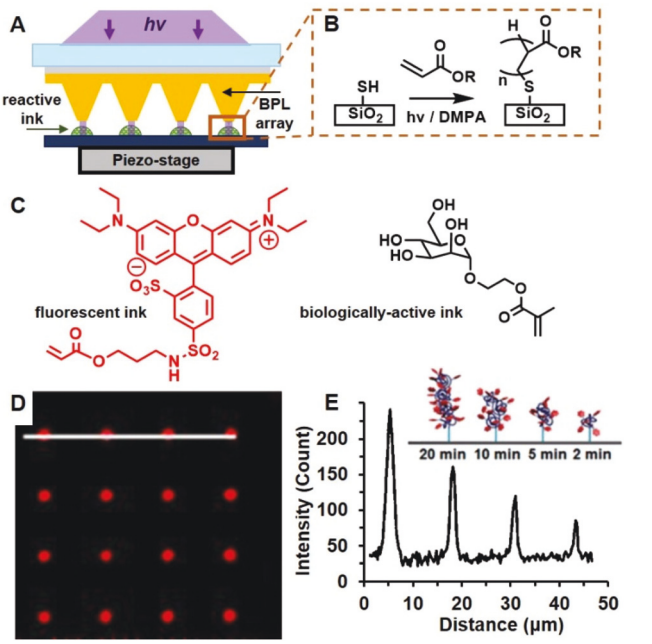

Fig. 4 (A) Beam pen lithography uses elastomeric tips coated in Au to deposit molecules onto the surface, then light passing through apertures in the beam pens exposes individual features in the pattern to initiate the photopolymerization from initiating groups on the surface. (B) Thiol–ene chemistry was used to immobilize alkene-labelled inks, and thiol-(meth)acrylate chemistry was used to polymerize acrylates from the thiol-terminated surface. (C) Two inks were immobilized to be characterized by fluorescence microscopy and to assess binding of polymers to GBPs. (D) Fluorescence microscopy image of a surface patterned with α-D-glucose methacrylate and incubated in a solution of fluorescently-labelled ConA. (E) Intensity profile of the features printed with different exposure times where the inset is a cartoon of the brush polymers' height variation as exposure times change.

analyzed *via* fluorescence microscopy (Fig. 4D) and AFM. We found that the thiol-labeled rhodamine only formed monolayers, whereas the fluorescence and height of the acrylate polymer brushes is dependent upon the irradiation time, showing that photoinduced propagation proceeded successfully and that the polymer height could be controlled precisely (Fig. 4E). Subsequently, the glycosylated monomer – α-D-glucose methacrylate – was polymerized with this approach, resulting in glycopolymer arrays, where the height of each glycopolymer pixel could be systematically varied. It was found that the glycopolymers could bind fluorescent ConA at concentrations several orders of magnitude lower than the monolayer glycan arrays. The higher sensitivity was attributed to the ability of the glycopolymers to capture the fluorescent lectin by way of biomimetic multivalent and cooperative binding modes. This work was the first report of the growth of grafted-from brush polymers with BPL, and showed that different height brushes could be grown at different pixels in a pattern through the spatiotemporal control of catalytic irradiation. Importantly, we found that increasing the dimensionality of the pattern by moving from 2D monolayer arrays to 3D polymer brush patterns resulted in the reproduction of biomimetic recognition that occurs on interfaces, which, in turn, leads to substantially stronger glycan–lectin recognition. Despite these advances, several additional capabilities would still need to be demonstrated to create arbitrary hypersurfaces. These include creating patterns with different compounds at different pixels, *i.e.* multiplexed patterning, and creating an arbitrary pattern over the entire surface rather than having a small pattern reproduced several times over the print area.

Liquid cells for multiplexed organic chemistry

Multiplexed soft-material micropatterning and nanopatterning is an ongoing challenge for SPL and any other patterning method. The inability to place different materials at arbitrary locations in the patterns renders the printing approaches inadequate for many envisioned applications, including sensors and displays, and overcoming this limitation required reimagining printer design. The SPL methods already discussed rely upon placing an ink onto a pen or pen array and transferring the ink to the surface *via* an aqueous meniscus. Several attempts have been made to create multiplexed patterns with these tips that do not rely on changing the printer design, and, as a result, the multiplexing capabilities are severely restricted. For example, by using the pen array mold as ink wells to dip the pen array into prior to patterning the inks, each tip could be loaded with a different ink.[115,149] The restriction, however, is that each tip prints only a single ink, and so different inks cannot be placed in close proximity. Alternatively, Fuchs *et al.* fabricated a multiplexed pattern by placing different inks onto different regions of polymer pen arrays, but they were limited to 5 inks in a pattern.[114] These examples illustrate that increasing the number of different compounds that could be patterned onto a single surface remained a challenge. So without making major modifications to the printer design, arbitrary multiplexing – where the chemical composition at any pixel in the surface could be arbitrarily controlled – would still not be achievable.

Our first attempt at solving this multiplexing challenge involved modifying the SPL printer architecture so that liquids can flow in and out of microfluidic channels that cover the printing area, allowing for ink exchange during printing. Photochemical reactions would then be used to immobilize molecules onto a surface. This approach represented a fundamental shift in SPL in two ways. The first is that reactions were now carried out in solution rather than in air. The second is that the tips were no longer used to deliver and pattern ink onto a surface, rather the reactive molecules were distributed throughout the reactive solution that coated the surface and the tips were used solely to localize the activation energy that drives the reaction forward. With this approach, materials of different compositions can be printed in close proximity in a single print by coordinating the spatiotemporal delivery of activation energy with the ink exchange. To do so, we designed a flow-through microfluidic device where inks were mixed in the reaction chamber and a beam pen array is lowered into a chamber within the microfluidics to localize light onto the surface (Fig. 5A), initiating a grafted-from photochemical polymerization (Fig. 5B). To demonstrate the capabilities of this architecture, two different fluorescently labeled acrylate inks (Fig. 5C) were sequentially pumped through the reaction chamber to graft brushes of different composition in close proximity on the same surface (Fig. 5D and E). The effect of multiple reaction variables on brush height, such as photoinitiatior concentration, light intensity, monomer/photoinitiator ratio, reaction time, solvent, and z-piezo extension, were explored systematically. Spots of methacrylate polymers functionalized with different fluorophores were printed with a separation of only a few micrometers. This work demonstrated our first approach to 4D printing, where the four independent dimensions are the x and y position, which are determined by the piezoelectric actuator stage, the height of each polymer feature (z), which is regulated by the illumination time at each pixel, and the chemical composition, which is controlled by the microfluidics. Despite demonstrating the proof-of-concept that SPL and microfluidics could be combined to create multiplexed polymer brush microarrays, we only succeeded in printing two different polymer brush pixels with each tip. This work, however, was a major step towards the goal of a dedicated HP printer because through this experimentation, we identified design flaws, including that light leaking through the transparent polymer pen arrays caused high background polymer growth, that the complexity of the microfluidics made it difficult to move the tip arrays with respect to the surface, and that the inks were not well mixed within the reaction chamber.

Capillary multiplexing and high-throughput reaction kinetics

In building a second generation, microfluidic-enabled SPL printer, we responded to lessons learned during the development of the first microfluidic cell by simplifying the fluid delivery to the reactive surface and introducing beam pen

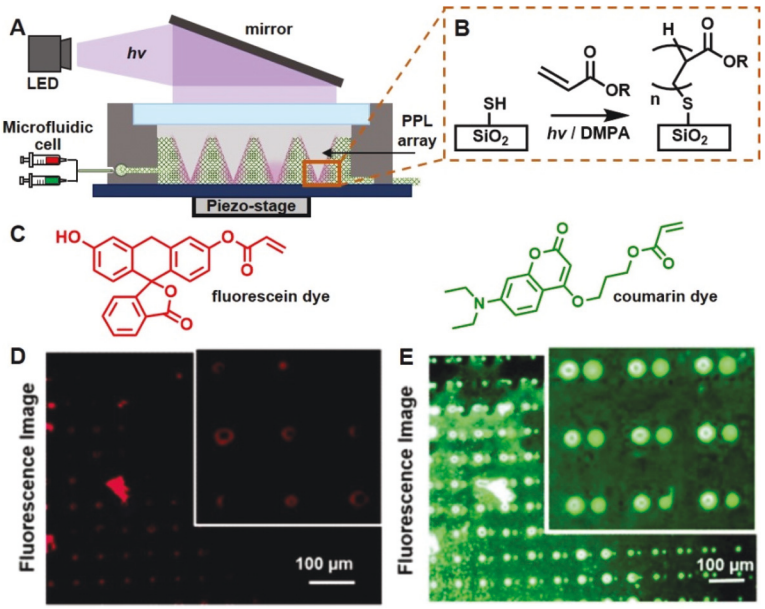

Fig. 5 (A) Multiplexed photochemical polymerization performed with polymer pen arrays in a fluid cell. Polymer pen arrays focus light through the tips onto the surface to induce grafted-from thiol-(meth)acrylate photochemical polymerizations. (B) Grafted-from thiol-(meth)acrylate from a thiol-terminated surface. (C) Polymers of two inks were grafted-from the surface in a single pattern as a result of the ability of the microfluidics to change inks during printing. (D) Fluorescence image of rhodamine (λ_{ex} = 522 nm, λ_{em} = 572 nm) patterned next to (E) coumarin (λ_{ex} = 354 nm, λ_{em} = 440 nm) on the same surface.

arrays to reduce off-target polymerization. Several changes were made to the printer architecture. The first of which was to swap the polymer pen arrays for beam pen arrays, where the Au coating blocks the light from illuminating areas of the surface outside of the pixels, thereby reducing off-site polymerization (Fig. 6A). In addition, the fluid printing cell was removed entirely, and, instead, the ink was first flowed through a microfluidic chaotic mixer that efficiently combines the various solutions into a homogenous ink, which is then flowed over the substrate, where capillary forces draw the printing solution between the tip arrays and the surface. In addition to being far simpler to implement, by removing the fluid cell from around the tip array, the movement of the tip arrays were not restricted.

To test the multiplexing capabilities of this printer we synthesized three different alkene-functionalized fluorophores (Fig. 6C). The inks were immobilized onto a thiol-functionalized surface by UV-light triggered photochemical thiol–ene reactions (Fig. 6B) between the thiol-terminated surface and the alkene-fluorophores in the solution that were sequentially introduced to the printing area. Capitalizing on the easy repositioning of the tips by the *x*,*y* piezo stage, the light that drives the reaction is easily repositioned so different fluorophores can be printed at different pixels. So by sequentially introducing a new ink, shining light on a pixel, moving the tip-arrays, and repeating the cycle as needed, multiplexed patterns are created by each tip in the beam pen array (Fig. 6D). This ability was confirmed by using the printer to print patterns with 9 unique colors by each pen by mixing the three different fluorophores in different ratios (Fig. 6E).

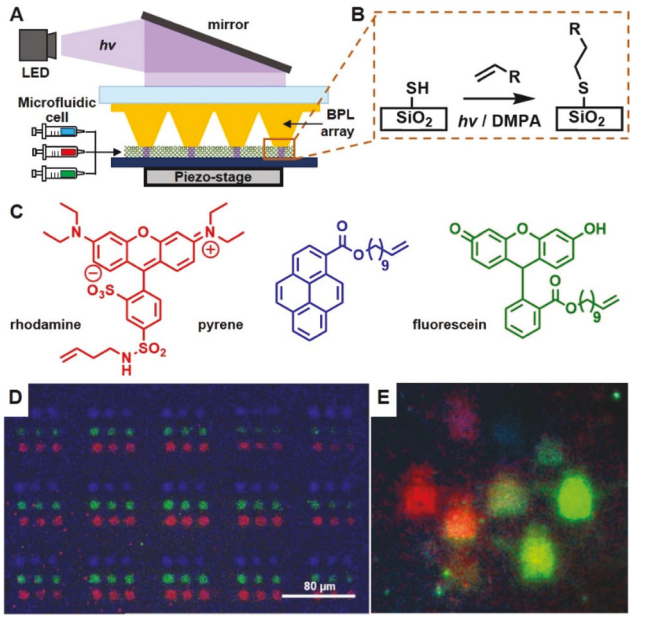

Fig. 6 (A) Microfluidic mixing in combination with beam pen arrays are used to focus light onto the surface to photochemically induce (B) thiol–ene click reactions between different alkene-labelled fluorophores and thiol-functionalized surfaces. (C) The three fluorescent dyes functionalized with alkenes that were patterned onto the thiol-terminated surfaces. (D) Multiplexed combinatorial patterning of three fluorescent dyes onto a single surface. (E) By mixing the inks in different ratios, features of 9 different colors were prepared.

We also showed how this easy mixing of inks and the ability to vary the irradiation time and intensity at each pixel could be used to address one of the biggest bottlenecks in surface chemistry, namely the inability to rapidly assess how different conditions affect reaction rates and yields. To do so, the effect of light intensity and exposure time on fluorescence intensity was studied systematically. A fluorescent ink was patterned into 5 × 5 arrays under continuous solution flow. The patterns were analyzed *via* fluorescence microscopy and the fluorescence for the 25 spots that were each printed under a different condition were tested. Because the same pattern is repeated by each tip, statistically significant printing data is produced in a single print, which also reduces error arising from batch-to-batch variability. In addition to providing a kinetic model for the surface reaction, this also led to a counterintuitive observation: while fluorescence increased with increasing irradiation time, as expected, fluorescence, on the other hand, decreased with increasing light intensity. The work in this report was crucial toward building a hypersurface printer, not only for providing a viable strategy towards multiplexing, but also for demonstrating the necessity for understanding the complexity of surface chemistry to achieve control over reaction yield. However, drawbacks to our multiplexing attempts persisted, such as the fact that each pen repeated the same pattern throughout, and we had not yet shown control over both chemical composition and the height simultaneously.

Capillary multiplexed glycan microarrays

To demonstrate the practical utility of these printing strategies, we sought to prepare glycan microarrays because, of all the common biological binding pairs, glycan-GBP recognition most often occurs at interfaces and is sensitively dependent upon surface structure.[150,151] Glycan microarrays, composed of carbohydrates patterned onto substrates, have become an invaluable tool for investigating the role of glycans and GBPs on cell adherence, motility, and signaling, which have important implications for therapeutics and diagnostics.[152–154] Despite the progress made in glycan microarray technology,[155–159] there is still a need to decrease feature sizes to increase probes per surface area, demonstrate facile immobilization chemistry that can be used for all glycans, and prepare high-throughput assays to understand GBP-glycan binding. As a demonstration of the utility of the new capillary-enabled microfluidic fluid exchange, we prepared a series of glycan microarrays to show how the exquisite control over surface chemistry could allow us to explore the subtleties of biological recognition. Specifically, we used a further modified version of the photochemical hypersurface printer (Fig. 7A) to prepare glycan microarrays. The major difference in this printer architecture compared to the one reported previously is that the beam pen arrays were removed, which makes printing substantially easier but each pixel on the surface had an edge length of ~4 μm. This was acceptable for the particular application because there was no need for smaller features, as these features were already a 100-fold reduction in area compared to the spots in conventional glycan microarrays.

To demonstrate the capabilities of this platform, we printed two different types of glycan microarrays: first we prepared a multiplexed glycan microarray, where multiple different glycans were immobilized onto a single substrate to study GBP specificity (Fig. 7B). In a second array, we varied systematically the density of pent-4-enyl-α-D-mannopyranoside (α-Man) to explore the effect of glycan surface density on GBP binding. The thiol–ene reaction was chosen because it proceeds photochemically with high yield and selectivity, we have shown that it is easily induced with our printer architectures, and alkenes are well known as glycan protecting groups and easily incorporated onto the anomeric (C1) carbon of carbohydrates, so these glycans were easy to obtain. Thus, we printed five different alkene-labelled glycans (α-mannose, α-galactose, β-galactose, β-glucose, α-glucose) onto a chip using thiol–ene photochemistry. To increase the throughput of the analysis of binding between GBPs and the printed arrays, we designed a microfluidic incubation chip which contained eleven 250 μm wide channels to support a different GBP solution in each channel. By placing the incubation chip on top of the printed area, the binding of eleven different GBP solutions to the five printed glycans was tested simultaneously. Binding assays were performed with two different fluorescently-labeled GBPs, FITC-Con A (fluorescein isothiocyanate-concanavalin A) (Fig. 7C) and rhodamine-RCA120 (rhodamine-labelled ricinus communis agglutinin I) (Fig. 7D). These two lectins were chosen because Con A is selective toward mannose and glucose, while RCA120 is selective toward galactose, and so by choosing these two GBPs we could explore whether natural GPB selectivity was maintained in our lectin arrays, and we found that it was. Thus, we showed that the miniaturized glycan array in combination with the incubation chip rapidly accelerates the study of glycan interaction, which is made possible because of reduced feature sizes.

Glycan-GBP recognition is typically weak in solution and relies upon multivalent and cooperative binding modes that occur on the surface to achieve strong and specific binding.[160] As such, the 2D structure of monolayer glycan microarrays plays a critical in recreating the recognition phenomena as they may occur at biological interfaces.[151] To this end, we prepared a second multiplexed monolayer glycan array to study how the surface density of α-Man would affect ConA binding to the array. This was accomplished by printing an array where α-Man was systematically diluted in the printed features with the biologically inert alkene, allyl alcohol, which could also be immobilized to the thiol-surface with the same photochemical thiol–ene click reaction. The ratio of the two alkenes – the glycan and the inert spacer – was controlled by simply varying their relative concentrations in the printing solution. The association between the glycans in this microarray and ConA was studied in the microfluidic incubation chip, where solutions with varying [ConA] were exposed to the features printed at varying glycan : spacer ratios. Fluorescence microscopy images of the resulting array provided data to analyze avidity,

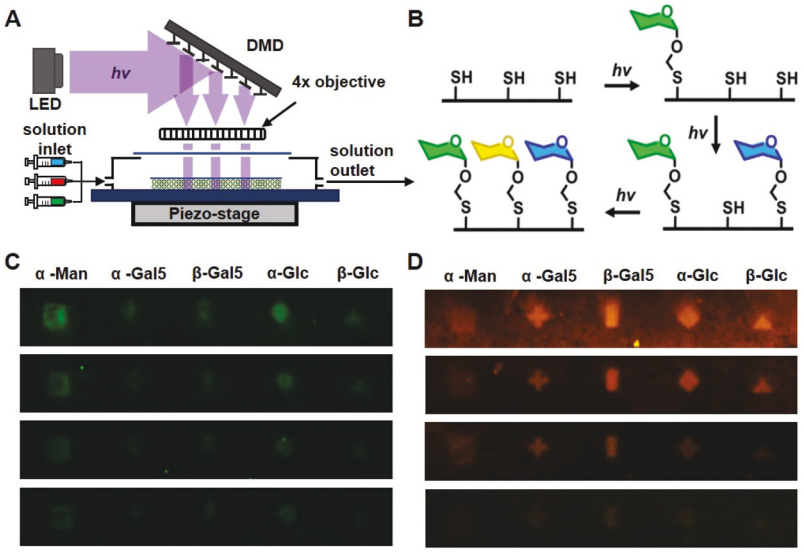

Fig. 7 (A) Printer equipped with a digital micromirror device (DMD) and microfluidic ink control for multiplexed patterning. (B) Thiol–ene chemistry was used to pattern different alkene labeled glycans onto thiol-functionalized surfaces. (C) Multiplexed glycan arrays fabricated by immobilizing alkene-labeled glycans onto to a thiol-functionalized surface. A microfluidic chip with 11 different channels was used to assay the binding of two GBPs, ConA and (D) the rhodamine-labelled, galactose-specific GBP (rhodamine-labelled ricinus communis agglutinin I) RCA120 at 4 different concentrations of each GBP for high through-put analysis of the specificities and binding affinities of the GBPs towards different immobilized glycans.

K_d, of ConA to the surface glycans for 8 different ConA concentrations and 11 different ink ratios. We found that K_d increases with decreasing mole fraction (χ) of α-Man, and we observed an abrupt decrease in fluorescence at $\chi = 0.2$. This observation can be explained by considering the average spacing between glycans. At $\chi = 0.2$, the glycan spacing is larger than the spacing between binding sites on ConA, and the GBP cannot bind to the surface multivalently, which is required for the ConA to remain on the surface, thus explaining the abrupt decrease in binding for $\chi \leq 0.2$. In addition to demonstrating the power of these printing tools in the context of glycobiology, this work was an important step in the path towards HP. First, we confirmed the ease with which multiplexing is accomplished with the 'capillary-flow' architecture. Second, the printing architecture used for this work removed the pen array altogether from the optical path, which increases the minimum feature edge-length to ~4 μm, although it also reduces significantly the complexity of printing. However, in these arrays the binding between the glycan microarrays and GBPs remained relatively weak, and so there is still a need in glycobiology for methods that recapitulate the 3D architecture of biological interfaces to capture accurately the dynamics of glycan recognition.

Arbitrary 3D polymer brush patterns

The next printing challenge we sought to address in our progress towards HP was to show that the polymer height could be independently controlled at any pixel across the surface, patterns which we refer to as variable height homopolymer patterns. To accomplish this feat, we used the DMD-equipped printer described above (Fig. 8A) to study the growth rates of the thiol-(meth)acrylate photopolymerization (TAP) (Fig. 8B), a reaction that is studied for tissue engineering,[161–164] creating hydrogels,[164,165] preparing glycan microarrays,[16,130] and controlling cell–substrate interactions.[162] Thus we reasoned that patterning using this polymerization could open many new opportunities in material science and biology, but the kinetics of the reaction were poorly understood and this reaction had never been used to create polymer brush arrays. To carry out this study, we leveraged the ability of the printer to vary the irradiation time independently at each pixel to carry out high throughput kinetic studies, whereby polymers were grown with different irradiation times at different pixels on the same surface. The effects the photocatalyst concentration, monomer concentration, and light intensity on feature height and growth rate were studied by varying printing time for each set of reaction conditions, and using AFM to determine feature height. Several important insights into the polymer kinetics were made as a result of the ability of this method to rapidly test >200 different reaction conditions. We found that feature heights increase linearly as exposure time and photocatalyst concentrations increase, then the growth plateaus at longer times, in-line with other studies on the growth kinetics of photopropagated grafted-from polymer brushes.[43,166,167] One observation that was unexpected was that, after a certain light intensity was reached, further increasing light intensity decreased growth rate, a phenomena that would not likely have been discovered without the high-throughput studies enabled by this platform. We were further able to show that propagation could be turned on and off by turning the light on and off (Fig. 8C), respectively, which is a key feature of reversible-deactivation radical propagation mechanisms (RDRP).[43]

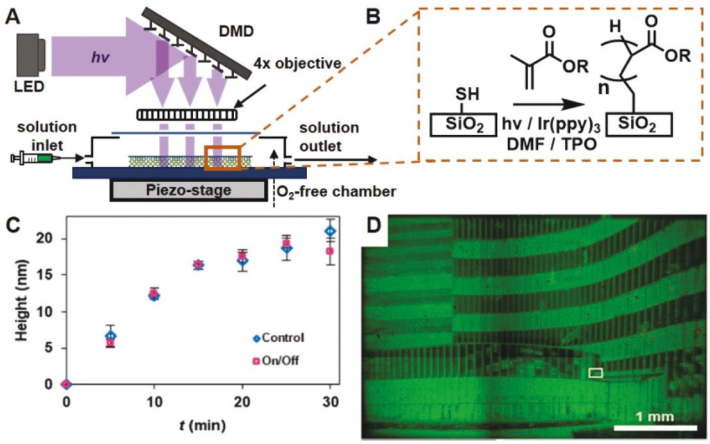

Fig. 8 (A) Hypersurface photolithography printer equipped with microfluidics, an inert printing chamber, and a CPU controlled DMD to direct light onto the surface. (B) Surface initiated thiol–acrylate photopolymerization. (C) Feature heights *vs.* *t* were compared from the on/off experiment (red squares) and the control experiment (blue squares) where features were exposed with continuous light intensity. (D) An image of the City University of New York's Advanced Science Research Center was patterned onto the surface.

This observation is an important validation of this approach because, prior to this study, the TAP had not been considered to be an RDRP. Another important demonstration achieved in this study was showing how a rigorous understanding of growth kinetics could be used to make arbitrary 3D patterns, where the polymer height at each pixel could be independently controlled. To do so, a black and white photograph was converted to a set of four binary images that correspond to different exposure times during patterning. Upon irradiating the surface with the four different images, the 3D polymer brush pattern in the shape of the photographic image was obtained, where light intensity in the original image was converted to polymer height in the variable height pattern (Fig. 8D). Thus, we had established that this printing architecture could create arbitrary 3D polymer brush patterns with micrometer-scale pixel edge lengths by combining the capillary-based printing architecture with advanced polymer chemistry, and the next challenge to be addressed involved creating arbitrary, multiplexed, polymer-brush patterns.

Polymer brush hypersurface photolithography

As the next step in printer evolution, we combined the grafted-from photopolymerization driven by light from a DMD – which provide precise control over height at each pixel – with capillary-flow multiplexing to control the composition of the monomers being propagated at each pixel (Fig. 9A). With the DMD-enabled printer architecture, we achieved true multiplexed polymer brush and copolymer brush hypersurfaces, where the monomer composition can be controlled in each voxel of the structure. To do so, we first used the printer to drive surface-initiated atom transfer radical photopolymerization (SI-ATRP, Fig. 9B). SI-ATRP was chosen because of its broad monomer compatibility[3,32,168–170] and because it performs reliably in a variety of different printing platforms.[36,37,171–176] A drawback of this reaction, however, is that O_2 and H_2O interfere with the propagation, so we designed an inert atmosphere chamber that surrounds the fluid cell. The propagation kinetics of SI-ATRP were understood by studying multiple different polymerization conditions in a single print to rapidly determine the relationship between irradiation time and polymer height. These data were then used to pattern a variable-height polymer brush image of the Statue of Liberty by the same method we patterned pictures with the thiol–acrylate polymerization (Fig. 9C). The successful image construction was confirmed *via* fluorescence microscopy and AFM.

Given the ability of this platform to both grow polymer brushes and change inks, we next set to demonstrate multiplexed polymer brush and block copolymer brush hypersurfaces, where, in the former, the composition of the polymer brush at any pixel can be varied arbitrarily and, in the latter, the composition can be controlled at any pixel and any voxel. In other words, we sought to use this printer to show that we could vary composition of the brush grafted at any position on the surface as well as along the chain. To create these polymer brush hypersurfaces, three different colored methacrylate monomers were prepared, and the propagation kinetics for each was studied independently to determine the relationship between irradiation time and brush height. By coordinating the DMD and microfluidics, a reproduction of a painting of the Barcelona skyline was printed (Fig. 9D), where the color and the brightness/height of each pixel was controlled by varying the composition of the monomer flowed into the fluid cell or the irradiation time, respectively. The pattern was then imaged using fluorescence microscopy, revealing the successful patterning of a polymer brush hypersurface, where the composition and height at each pixel over a large surface could be arbitrarily patterned.

Although it would be difficult, this same polymer brush pattern could be prepared using a series of photomasks, where each photomask prints a pattern composed of polymer

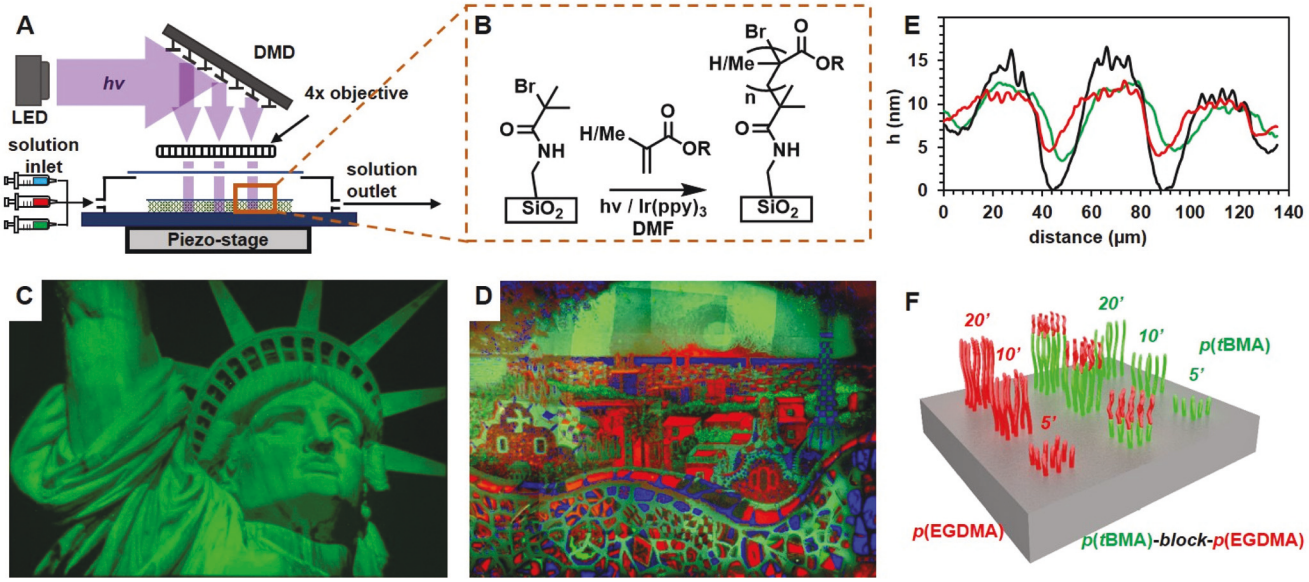

Fig. 9 (A) Hypersurface photolithography printer equipped with microfluidics for multiplexing, an inert atmosphere printing chamber, and a DMD to direct light onto the surface. (B) Surface initiated atom transfer radical photopolymerization. (C) A fluorescent 3D polymer brush image of the Statue of Liberty. (D) A painting of Barcelona composed of three different colored fluorescent brush copolymers. (E) Average height profiles of p(*t*BMA) (green), p(EGMA) (red), and block-copolymers (black). (F) Cartoon depicts an array composed of p(*t*BMA) brush features (green) and p(EGMA) brushes (red) printed at 5, 10 and 20 min. Block-copolymers were patterned with p(*t*BMA) and p(EGMA) in middle row at 5, 10 and 20 min.

brushes of a specific height and composition. There is, however, no current microfabrication method that can create arbitrary block copolymer hypersurfaces, where the composition of blocks and block lengths at each pixel could be independently varied. The problem with attempting to make copolymer brush hypersurfaces using a series of photomasks is that each photomask would have to be aligned precisely, and as a result of limitations with respect to realignment precision, it is extremely difficult to print one microscale feature directly onto another. In addition, growing block copolymers requires maintaining the living chain ends, and so masks would have to be changed while maintaining an inert atmosphere, which adds additional complications to the printing process. Using microfluidics to introduce new inks and the DMD to illuminate the surface circumvents the needs for alignment between introducing new inks and an inert atmosphere is easily maintained. To change composition along a chain, a new ink is flowed in, and the correct mirror is simply turned back on, and the whole process takes place under inert atmosphere to ensure the chain ends remain living. To this end, ethylene glycol dimethacylate (EGDMA) and *tert*-butyl methacrylate (*t*BMA), were printed to form pixels of homopolymer and block copolymer brushes that were analyzed by AFM to measure heights and confirm the formation of EGDMA-*block*-*t*BMA copolymer brushes (Fig. 9E and F). With this HP technology fully realized, we sought to demonstrate how the rapid chemical optimization and advanced printing capabilities could lead to new devices and chemistries that would be difficult or altogether impossible to implement in other printing platforms.

Stimuli responsive 6D hypersurfaces

Polymer brush films and polymer brush patterns are increasingly important in many aspects of science and technology – including in coatings,[177] sensors,[178] and responsive surfaces[179–182] – and are the subject of substantial research in materials science. Two major current challenges in this field include: (1) the difficulty in understanding how reaction conditions affect polymer brush growth rates and heights, and (2) the inability of printing platforms to independently control the chemical composition of the polymer brush in each voxel so that different block copolymers can be created in each voxel with micrometer-scale feature dimensions. In this report, we showed the multidimensional printing capability of the hypersurface printer to create patterns, where we can control the x, y position, the height, the composition, the response to light, and the response to heat in each voxel, which, as a result, we term 6D hypersurfaces. Some of the polymer brushes in this pattern contain as many as four different blocks, where the height and chemical composition along the chain is controlled precisely. This 6D printing was demonstrated by printing orthogonal images within the same pattern – when exposed to light one image is revealed and when exposed to heat a different image emerges. The patterns that were prepared for these hidden images to emerge illustrate how our new printer makes the fabrication of such patterns almost trivial.

With the HP printer (Fig. 10A) we first varied propagation conditions, resulting in a comprehensive understanding of the grafted-from polymerization of the monomers *N*,*N*-dimethylacrylamide (DMA) and *N*-isopropylacrylamide (NIPAM) when

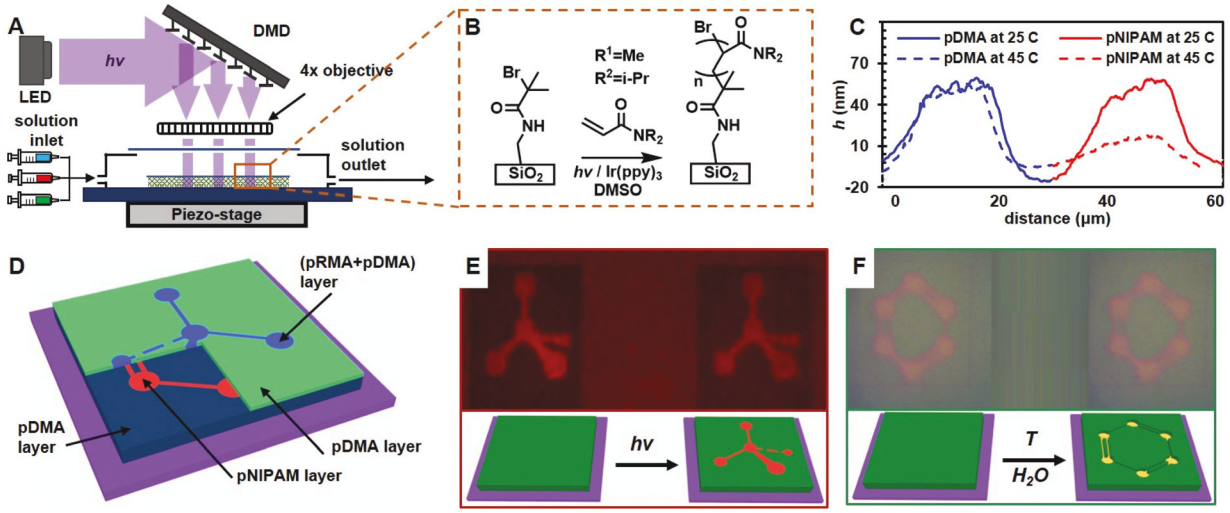

Fig. 10 (A) Hypersurface photolithography was used to pattern stimuli responsive surfaces composed of (B) pNIPAM and pDMA brushes. (C) The thermoresponsive behavior of pNIPAM and pDMA was studied by heating patterns containing both polymer brush in H_2O. (D) Structure of the 6D hidden image, which was made by multiplexed patterning of pNIPAM, pDMA, and a copolymer of pDMA and pRMA. (E) A fluorescent hidden image of a tetrahedral carbon is revealed upon exposure to 530–550 nm light. (F) A hidden image of benzene is revealed upon heating the 6D pattern above the pNIPAM LCST in H_2O.

propagated from surface-bound initiators using SI-ATRP (Fig. 10B). These two monomers were chosen because polymer brushes of pNIPAM collapse in water heated above the lowest critical solution temperature (LCST) of pNIPAM, while pDMA brushes do not collapse, thereby providing a method to conceal a message that is revealed upon pNIPAM collapse. Once the growth rates were understood, experiments were performed to quantify the swelling-collapsing transition of the pNIPAM brushes in response to changes in temperature to ensure that an appreciable change in height would occur and that the temperature-responsive images could be easily observed optically. The collapsing coefficient was determined in H_2O by measuring the height of pNIPAM and pDMA at 25 °C and at 45 °C with an AFM, which were below and above the pNIPAM LCST, respectively (Fig. 10C). After understanding the kinetics and the collapsing coefficient of pNIPAM, we took advantage of the living nature of the SI-ATRP, and the ability to introduce reagents sequentially into the printing chamber with the integrated microfluidics by first creating a pattern where pDMA and pNIPAM were grown to the same height. Upon heating the pattern in H_2O, a change in height was observed only in the pixels patterned with pNIPAM, thereby revealing a secret message. Subsequently, we designed 6D hypersurfaces (Fig. 10D) that revealed different images when heated or when exposed to UV light. While the chain ends remained living, a printing solution of DMA doped with RMA was introduced into the fluid cell to create a short copolymer, which would place a fluorescent "hidden message" on top of the height-responsive pattern. Under ambient conditions no pattern is seen, whereas upon exposure to UV light a tetrahedral carbon is observed (Fig. 10E). Alternatively, upon heating the same pattern above the pNIPAM LSCT in H_2O, a benzene ring is revealed (Fig. 10D). With this work we demonstrated the major benefits of HP, in that complex and functional polymer brush films can be easily prepared, while reducing substantially research efforts and costs.

Glycopolymer microarrays with sub-femtomolar avidity for glycan binding proteins

The glycocalyx is a dense layer of glycans on the surface of all eukaryotic cells that is approximately 100 nm–1 μm thick, where glycan-GBP interactions occur.[183] To reproduce the binding interactions that occur in biology and to detect GBPs at biologically-relevant concentrations, glycan microarrays should reflect more accurately the multivalent presentation of glycans in the glycocalyx. Ideally, the approaches to create the glycan arrays should enable the facile integration of widely available glycans onto multivalent scaffolds. In an effort to create better surfaces for sensors, coatings, and cell growth, we leveraged the accelerated reaction discovery enabled by HP to develop an entirely new photoinitiated polymerization, that we termed 'grafted-to/grafted-from radical photopolymerization' (GTGFRP) (Fig. 11B), where functional groups are grafted-to a polymer as it grows grafted-from a surface.[16] In our previous report, we used thiol-functionalized surfaces to initiate the TAP reaction.[143] Here, we built upon this reaction but made several critical changes, including the addition of pentaerythritol tetrakis(3-mercaptopropionate) (PETT) (Fig. 11C) as a monomer, which leads to a highly cross-linked polymer that continues to propagate under continuous light exposure under ambient conditions and without metal catalyst. These changes removed the necessity of an inert environment, increased substantially the maximum feature height, from <100 nm to >20 μm, and provides a means to incorporate functional groups either during or post-polymerization. We used this new GTGFRP chemistry for patterning cross-linked polymer

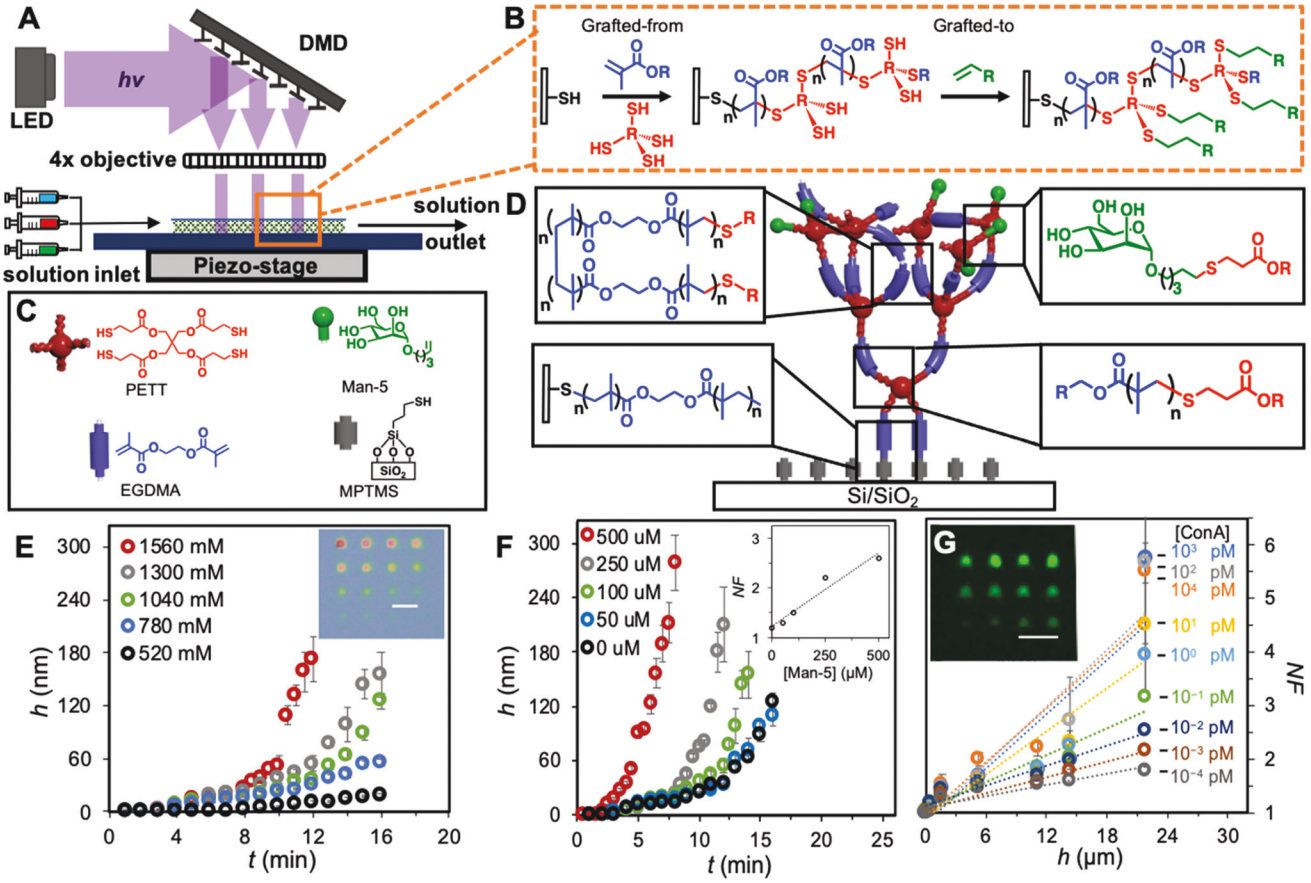

Fig. 11 (A) Hypersurface photolithography was used to patterned copolymer brushes from surfaces. (B) Grafted-to/grafted-from radical photopolymerization (GTGFRP) from a thiol-terminated surface. (C) Constituents of the glycopolymer brush represented in (D) prepared by the GTGFRP reaction. (D) Model of the glycopolymer brush formed by the GTGFRP and the chemical bonds that occur. (E) Growth rates of the glycopolymer brushes were studied by systematically varying monomer concentration ([EGDMA]) and light exposure time, *t*. An optical image of a 4 × 4 pattern is shown in the inset with a scale bar of 100 μm. (F) Relationship between height, *h*, and irradiation time for glycopolymers composed of EGDMA, PETT. The concentration of α-Man was varied systematically to understand how it affected growth rate. The inset shows the effect varying [Man-5] on normalized fluorescence (NF) with polymer brushes with heights of 110 ± 10 nm. (G) Binding study performed by varying ConA concentration on surfaces with glycopolymer brushes with varying *h*. The inset is fluorescence microscopy of ConA bound to Man-5 glycopolymers with a scale bar of 100 μm.

brushes. We grew surface copolymers containing EGDMA and PETT from thiol-functionalized surfaces (Fig. 11D). The kinetics of this polymerization experiment were studied by patterning a surface with each spot representing a different exposure time. Polymer heights were studied systematically by varying both monomer concentrations (Fig. 11E), photoinitiator concentrations, light intensity, and exposure time so that the height of the cross-linked polymer brushes at each feature could be precisely controlled.

Once the kinetic data for the copolymer brush composed of EGDMA and PETT monomers was understood, we added a new monomer to the printing solution, α-Man, the same alkene labelled mannose used in our previous reports.[14,15] This resulted in a GTGFRP reaction in which the glycans are grafted-to the thiols of a PETT–EGDMA polymer chain as it grows grafted-from a surface. The resulting glycan microarrays, in which both brush height and glycan density were varied, were used to explore systematically the role of glycan grafting density and polymer height on K_d. We observed that as the [α-Man] increased in the printing solution, the grafting density of α-Man on the polymer brush would also increase (Fig. 11F). Subsequently, vertical lines were patterned onto a surface with different growth times and a glycan concentration of 500 μM, where feature heights from the polymers varied from 10 nm to 20 μm. The same 11-channel incubation chip described above was used for high throughput binding assays, where the concentrations of fluorescently-labelled ConA was varied from 10^4–10^{-4} pM. Analysis of the resulting fluorescent images revealed K_d values as low as 0.3 fM, the strongest binding between a mannoside and ConA ever observed in a glycan microarray (Fig. 11F). We attribute this strong binding to the multivalent and cooperative interactions that occur between ConA and the multivalent glycopolymer brushes. Thus, in this report we showed how HP could lead to the discovery and optimization of new surface chemistry, and then used this combination of advanced printing architectures and surface

chemistry to create new glycan microarray architecture for the ultrasensitive detections of GBPs, a result that is bound to have a substantial impact on the rapidly growing field of glycobiology.

Conclusions

Here we showed the development of chemistries and instrumentation to pattern molecules onto surfaces with control over position, height, and composition, while maintaining micrometer-scale voxels, all resulting in the development of HP. This new printing strategy is a versatile method for multi-dimensional printing of soft-matter at the microscale and nanoscale. This could not have been done without advances in chemistry and instrumentation, which have both been a major bottleneck that has slowed discovery in chemistry and materials science. The ability to easily functionalize surfaces with such with such precision widens the spectrum of applications of patterns of grafted-from polymer brushes[23,184–186] to include fundamental studies of polymer chemistry,[187–189] directing and controlling protein adsorption and cell adhesion,[190,191] chemical sensing,[192] analytical devices that use combinatorial microarrays,[193] micro- and nanofluidic devices,[194,195] stimuli responsive materials,[17,18] luminescent surfaces,[170] and biomimetic architectures.[196] As we continue developing this printing platform, future work will focus on further reducing feature dimensions, automating printing, and increasing the substrate and reaction generality of this printing approach.

Conflicts of interest

The authors declare no competing financial interests.

Acknowledgements

This work was supported by funding from the Air Force Office of Scientific Research (FA9550-19-1-0356), the National Science Foundation (DBI-2032176), and the Department of Defense (MURI 15RT0675).

Notes and references

1 S. T. Milner, Polymer Brushes, *Science*, 1991, **251**(4996), 905–914.
2 W.-L. Chen, R. Cordero, H. Tran and C. K. Ober, 50th Anniversary Perspective: Polymer Brushes: Novel Surfaces for Future Materials, *Macromolecules*, 2017, **50**(11), 4089–4113.
3 J. O. Zoppe, N. C. Ataman, P. Mocny, J. Wang, J. Moraes and H.-A. Klok, Surface-Initiated Controlled Radical Polymerization: State-of-the-Art, Opportunities, and Challenges in Surface and Interface Engineering with Polymer Brushes, *Chem. Rev.*, 2017, **117**(3), 1105–1318.
4 A. B. Braunschweig and L. Hartmann, *Nanolithography of Biointerfaces: Faraday Discussion 219*, Royal Society of Chemistry, 2019, vol. 219, pp. 262–275.
5 Z. A. Page, B. Narupai, C. W. Pester, R. Bou Zerdan, A. Sokolov, D. S. Laitar, S. Mukhopadhyay, S. Sprague, A. J. McGrath, J. W. Kramer, P. Trefonas and C. J. Hawker, Novel Strategy for Photopatterning Emissive Polymer Brushes for Organic Light Emitting Diode Applications, *ACS Cent. Sci.*, 2017, **3**(6), 654–661.
6 C. W. Pester, J. E. Poelma, B. Narupai, S. N. Patel, G. M. Su, T. E. Mates, Y. Luo, C. K. Ober, C. J. Hawker and E. J. Kramer, Ambiguous anti-fouling surfaces: Facile synthesis by light-mediated radical polymerization, *J. Polym. Sci., Part A: Polym. Chem.*, 2016, **54**(2), 253–262.
7 K. Jung, N. Corrigan, M. Ciftci, J. Xu, S. E. Seo, C. J. Hawker and C. Boyer, Designing with Light: Advanced 2D, 3D, and 4D Materials, *Adv. Mater.*, 2020, **32**(18), 1903850.
8 H. Hou, K. Hu, H. Lin, J. Forth, W. Zhang, T. P. Russell, J. Yin and X. Jiang, Reversible Surface Patterning by Dynamic Crosslink Gradients: Controlling Buckling in 2D, *Adv. Mater.*, 2018, **30**(36), 1803463.
9 Y. S. Zholdassov, D. J. Valles, S. Uddin, J. Korpanty, N. C. Gianneschi and A. B. Braunschweig, Orthogonal Images Concealed Within a Responsive 6-Dimensional Hypersurface, *Adv. Mater.*, 2021, **33**(21), 2100803.
10 V. M. Runge, W. R. Nitz, M. Trelles and F. L. Goerner, *Physics of Clinical MR Taught Through Images*, Thieme, New York, 3rd edn, 2014.
11 J. Lee, *Curves and Hypersurfaces in Euclidean Space. Manifolds and Differential Geometry*, Providance: American Mathematical Society, 2009.
12 S. Tibbits, 4D Printing: Multi-Material Shape Change, *Archit. Des.*, 2014, **84**(1), 116–121.
13 G. A. Sydney, E. A. Matsumoto, R. G. Nuzzo, L. Mahadevan and J. A. Lewis, Biomimetic 4D printing, *Nat. Mater.*, 2016, **15**(4), 413–418.
14 D. J. Valles, Y. Naeem, C. Carbonell, A. M. Wong, D. R. Mootoo and A. B. Braunschweig, Maskless Photochemical Printing of Multiplexed Glycan Microarrays for High-Throughput Binding Studies, *ACS Biomater. Sci. Eng.*, 2019, **5**(6), 3131–3138.
15 D. J. Valles, Y. Naeem, A. Y. Rozenfeld, R. W. Aldasooky, W. Rawan, A. M. Wong, C. Carbonell, D. R. Mootoo and A. B. Braunschweig, Multivalent binding of concanavalin A on variable-density mannoside microarrays, *Faraday Discuss.*, 2019, **219**, 77–89.
16 D. J. Valles, Y. S. Zholdassov, J. Korpanty, S. Uddin, Y. Naeem, D. R. Mootoo, N. C. Gianneschi and A. B. Braunschweig, Glycopolymer Microarrays with Sub-Femtomolar Avidity for Glycan Binding Proteins Prepared by Grafted-To/Grafted-From Photopolymerizations, *Angew. Chem.*, 2021, **60**(37), 20350–20357.

17 C. Lu and M. W. Urban, Stimuli-responsive polymer nanoscience: Shape anisotropy, responsiveness, applications, *Prog. Polym. Sci.*, 2018, **78**, 24–46.
18 Y. Tu, F. Peng, X. Sui, Y. Men, P. B. White, J. C. M. van Hest and D. A. Wilson, Self-propelled supramolecular nanomotors with temperature-responsive speed regulation, *Nat. Chem.*, 2016, **9**, 480.
19 X. Liao, K. A. Brown, A. L. Schmucker, G. Liu, S. He, W. Shim and C. A. Mirkin, Desktop nanofabrication with massively multiplexed beam pen lithography, *Nat. Commun.*, 2013, **4**(1), 2103.
20 B. W. Maynor, S. F. Filocamo, M. W. Grinstaff and J. Liu, Direct-Writing of Polymer Nanostructures: Poly(thiophene) Nanowires on Semiconducting and Insulating Surfaces, *J. Am. Chem. Soc.*, 2002, **124**(4), 522–523.
21 O. Azzaroni, Z. Zheng, Z. Yang and W. T. S. Huck, Polyelectrolyte Brushes as Efficient Ultrathin Platforms for Site-Selective Copper Electroless Deposition, *Langmuir*, 2006, **22**(16), 6730–6733.
22 Z. Nie and E. Kumacheva, Patterning surfaces with functional polymers, *Nat. Mater.*, 2008, **7**(4), 277–290.
23 X. Zhou, X. Liu, Z. Xie and Z. Zheng, 3D-patterned polymer brush surfaces, *Nanoscale*, 2011, **3**(12), 4929–4939.
24 B. Balakrishnan and R. Banerjee, Biopolymer-Based Hydrogels for Cartilage Tissue Engineering, *Chem. Rev.*, 2011, **111**(8), 4453–4474.
25 C. Carbonell, D. Valles, A. M. Wong, A. S. Carlini, M. A. Touve, J. Korpanty, N. C. Gianneschi and A. B. Braunschweig, Polymer brush hypersurface photolithography, *Nat. Commun.*, 2020, **11**(1), 1244.
26 M. J. Madou, *Fundamentals of microfabrication: the science of miniaturization*, CRC Press, Boca Raton, Fla, 2nd edn, 2002 ©2002: 2002.
27 C. Carbonell and A. B. Braunschweig, Toward 4D Nanoprinting with Tip-Induced Organic Surface Reactions, *Acc. Chem. Res.*, 2017, **50**(2), 190–198.
28 X. Liu, C. Carbonell and A. B. Braunschweig, Towards scanning probe lithography-based 4D nanoprinting by advancing surface chemistry, nanopatterning strategies, and characterization protocols, *Chem. Soc. Rev.*, 2016, **45**(22), 6289–6310.
29 A. B. Braunschweig, F. Huo and C. A. Mirkin, Molecular printing, *Nat. Chem.*, 2009, **1**(5), 353–358.
30 W. Liu, X. Liu, P. Ge, L. Fang, S. Xiang, X. Zhao, H. Shen and B. Yang, Hierarchical-Multiplex DNA Patterns Mediated by Polymer Brush Nanocone Arrays That Possess Potential Application for Specific DNA Sensing, *ACS Appl. Mater. Interfaces*, 2015, **7**(44), 24760–24771.
31 Z. Xie, T. Gan, L. Fang and X. Zhou, Recent progress in creating complex and multiplexed surface-grafted macromolecular architectures, *Soft Matter*, 2020, **16**(38), 8736–8759.
32 M. Fromel, M. Li and C. W. Pester, Surface Engineering with Polymer Brush Photolithography, *Macromol. Rapid Commun.*, 2020, **41**(18), 2000177.
33 H. Takahashi, M. Nakayama, K. Itoga, M. Yamato and T. Okano, Micropatterned Thermoresponsive Polymer Brush Surfaces for Fabricating Cell Sheets with Well-Controlled Orientational Structures, *Biomacromolecules*, 2011, **12**(5), 1414–1418.
34 D. Bontempo and H. D. Maynard, Streptavidin as a macroinitiator for polymerization: in situ protein-polymer conjugate formation, *J. Am. Chem. Soc.*, 2005, **127**(18), 6508–6509.
35 K. L. Heredia, D. Bontempo, T. Ly, J. T. Byers, S. Halstenberg and H. D. Maynard, In Situ Preparation of Protein−"Smart" Polymer Conjugates with Retention of Bioactivity, *J. Am. Chem. Soc.*, 2005, **127**(48), 16955–16960.
36 R. Barbey, L. Lavanant, D. Paripovic, N. Schüwer, C. Sugnaux, S. Tugulu and H.-A. Klok, Polymer Brushes via Surface-Initiated Controlled Radical Polymerization: Synthesis, Characterization, Properties, and Applications, *Chem. Rev.*, 2009, **109**(11), 5437–5527.
37 B. P. Fors and C. J. Hawker, Control of a Living Radical Polymerization of Methacrylates by Light, *Angew. Chem., Int. Ed.*, 2012, **51**(35), 8850–8853.
38 F. A. Leibfarth, K. M. Mattson, B. P. Fors, H. A. Collins and C. J. Hawker, External Regulation of Controlled Polymerizations, *Angew. Chem., Int. Ed.*, 2013, **52**(1), 199–210.
39 N. J. Treat, B. P. Fors, J. W. Kramer, M. Christianson, C.-Y. Chiu, J. Read de Alaniz and C. J. Hawker, Controlled Radical Polymerization of Acrylates Regulated by Visible Light, *ACS Macro Lett.*, 2014, **3**(6), 580–584.
40 J. E. Poelma, B. P. Fors, G. F. Meyers, J. W. Kramer and C. J. Hawker, Fabrication of Complex Three-Dimensional Polymer Brush Nanostructures through Light-Mediated Living Radical Polymerization, *Angew. Chem., Int. Ed.*, 2013, **52**(27), 6844–6848.
41 K. Satoh, J. E. Poelma, L. M. Campos, B. Stahl and C. J. Hawker, A facile synthesis of clickable and acid-cleavable PEO for acid-degradable block copolymers, *Polym. Chem.*, 2012, **3**(7), 1890–1898.
42 J. Yan, B. Li, F. Zhou and W. Liu, Ultraviolet Light-Induced Surface-Initiated Atom-Transfer Radical Polymerization, *ACS Macro Lett.*, 2013, **2**(7), 592–596.
43 M. Li, M. Fromel, D. Ranaweera, S. Rocha, C. Boyer and C. W. Pester, SI-PET-RAFT: Surface-Initiated Photoinduced Electron Transfer-Reversible Addition–Fragmentation Chain Transfer Polymerization, *ACS Macro Lett.*, 2019, **8**(4), 374–380.
44 B. D. Gates, Q. Xu, M. Stewart, D. Ryan, C. G. Willson and G. M. Whitesides, New Approaches to Nanofabrication: Molding, Printing, and Other Techniques, *Chem. Rev.*, 2005, **105**(4), 1171–1196.
45 X. Younan and G. M. Whitesides, Soft lithography, *Annu. Rev. Mater. Sci.*, 1998, **28**(1), 153–184.
46 G. M. Whitesides, E. Ostuni, S. Takayama, X. Jiang and D. E. Ingber, Soft Lithography in Biology and Biochemistry, *Annu. Rev. Biomed. Eng.*, 2001, **3**(1), 335–373.

47 Y. Xia, J. A. Rogers, K. E. Paul and G. M. Whitesides, Unconventional Methods for Fabricating and Patterning Nanostructures, *Chem. Rev.*, 1999, **99**(7), 1823–1848.
48 O. Azzaroni, S. E. Moya, A. A. Brown, Z. Zheng, E. Donath and W. T. S. Huck, Polyelectrolyte Brushes as Ink Nanoreservoirs for Microcontact Printing of Ionic Species with Poly(dimethyl siloxane) Stamps, *Adv. Funct. Mater.*, 2006, **16**(8), 1037–1042.
49 G. Liu, S. H. Petrosko, Z. Zheng and C. A. Mirkin, Evolution of Dip-Pen Nanolithography (DPN): From Molecular Patterning to Materials Discovery, *Chem. Rev.*, 2020, **120**(13), 6009–6047.
50 G. Liu, M. Hirtz, H. Fuchs and Z. Zheng, Development of Dip-Pen Nanolithography (DPN) and Its Derivatives, *Small*, 2019, **15**(21), 1900564.
51 K. Salaita, Y. Wang and C. A. Mirkin, Applications of dip-pen nanolithography, *Nat. Nanotechnol.*, 2007, **2**, 145–155.
52 D. S. Ginger, H. Zhang and C. A. Mirkin, The Evolution of Dip-Pen Nanolithography, *Angew. Chem., Int. Ed.*, 2004, **43**(1), 30–45.
53 Y. Xia and G. M. Whitesides, Use of controlled reactive spreading of liquid alkanethiol on the surface of gold to modify the size of features produced by microcontact Printing, *J. Am. Chem. Soc.*, 1995, **117**(11), 3274–3275.
54 M. Mrksich, C. S. Chen, Y. Xia, L. E. Dike, D. E. Ingber and G. M. Whitesides, Controlling cell attachment on contoured surfaces with self-assembled monolayers of alkanethiolates on gold, *Proc. Natl. Acad. Sci. U. S. A.*, 1996, **93**(20), 10775–10778.
55 J. L. Wilbur, A. Kumar, H. A. Biebuyck, E. Kim and G. M. Whitesides, Microcontact printing of self-assembled monolayers: applications in microfabrication, *Nanotechnology*, 1996, **7**(4), 452–457.
56 S. A. Lange, V. Benes, D. P. Kern, J. K. H. Hörber and A. Bernard, Microcontact Printing of DNA Molecules, *Anal. Chem.*, 2004, **76**(6), 1641–1647.
57 D. I. Rozkiewicz, J. Gierlich, G. A. Burley, K. Gutsmiedl, T. Carell, B. J. Ravoo and D. N. Reinhoudt, Transfer Printing of DNA by "Click" Chemistry, *ChemBioChem*, 2007, **8**(16), 1997–2002.
58 C. Thibault, V. Le Berre, S. Casimirius, E. Trévisiol, J. François and C. Vieu, Direct microcontact printing of oligonucleotides for biochip applications, *J. Nanobiotechnol.*, 2005, **3**(1), 7.
59 D. I. Rozkiewicz, Y. Kraan, M. W. T. Werten, F. A. de Wolf, V. Subramaniam, B. J. Ravoo and D. N. Reinhoudt, Covalent Microcontact Printing of Proteins for Cell Patterning, *Chem. – Eur. J.*, 2006, **12**(24), 6290–6297.
60 A. Bernard, J. P. Renault, B. Michel, H. R. Bosshard and E. Delamarche, Microcontact Printing of Proteins, *Adv. Mater.*, 2000, **12**(14), 1067–1070.
61 E. E. Ross, J. R. Joubert, R. J. Wysocki, K. Nebesny, T. Spratt and D. F. O'Brie, Patterned Protein Films on Poly(lipid) Bilayers by Microcontact Printing, *Biomacromolecules*, 2006, **7**(5), 1393–1398.
62 J. S. Hovis and S. G. Boxer, Patterning and Composition Arrays of Supported Lipid Bilayers by Microcontact Printing, *Langmuir*, 2001, **17**(11), 3400–3405.
63 A. T. A. Jenkins, N. Boden, R. J. Bushby, S. D. Evans, P. F. Knowles, R. E. Miles, S. D. Ogier, H. Schönherr and G. J. Vancso, Microcontact Printing of Lipophilic Self-Assembled Monolayers for the Attachment of Biomimetic Lipid Bilayers to Surfaces, *J. Am. Chem. Soc.*, 1999, **121**(22), 5274–5280.
64 K. Godula, D. Rabuka, K. T. Nam and C. R. Bertozzi, Synthesis and Microcontact Printing of Dual End-Functionalized Mucin-like Glycopolymers for Microarray Applications, *Angew. Chem., Int. Ed.*, 2009, **48**(27), 4973–4976.
65 C. Wendeln, A. Heile, H. F. Arlinghaus and B. J. Ravoo, Carbohydrate Microarrays by Microcontact Printing, *Langmuir*, 2010, **26**(7), 4933–4940.
66 K. Godula, D. Rabuka, K. T. Nam and C. R. Bertozzi, Synthesis and Microcontact Printing of Dual End-Functionalized Mucin-like Glycopolymers for Microarray Applications (vol 48, pg 4973, 2009), *Angew. Chem., Int. Ed.*, 2012, **51**(32), 7881–7881.
67 V. Santhanam and R. P. Andres, Microcontact Printing of Uniform Nanoparticle Arrays, *Nano Lett.*, 2004, **4**(1), 41–44.
68 S.-T. Han, Y. Zhou, Z.-X. Xu, L.-B. Huang, X.-B. Yang and V. A. L. Roy, Microcontact Printing of Ultrahigh Density Gold Nanoparticle Monolayer for Flexible Flash Memories, *Adv. Mater.*, 2012, **24**(26), 3556–3561.
69 H. Xu, X. Y. Ling, J. van Bennekom, X. Duan, M. J. W. Ludden, D. N. Reinhoudt, M. Wessling, R. G. H. Lammertink and J. Huskens, Microcontact Printing of Dendrimers, Proteins, and Nanoparticles by Porous Stamps, *J. Am. Chem. Soc.*, 2009, **131**(2), 797–803.
70 T. Kaufmann and B. J. Ravoo, Stamps, inks and substrates: polymers in microcontact printing, *Polym. Chem.*, 2010, **1**(4), 371–387.
71 J. J. Brondijk, X. Li, H. B. Akkerman, P. W. M. Blom and B. de Boer, Microcontact printing of self-assembled monolayers to pattern the light-emission of polymeric light-emitting diodes, *Appl. Phys. A*, 2009, **95**(1), 1–5.
72 M. Konig, K. Bock and G. Klink, Micro-contact printing of OTFT on polymer foils, in *2009 59th Electronic Components and Technology Conference*, 26–29 May 2009, 2009, pp. 1322–1324.
73 M. Ikawa, T. Yamada, H. Matsui, H. Minemawari, J. y. Tsutsumi, Y. Horii, M. Chikamatsu, R. Azumi, R. Kumai and T. Hasegawa, Simple push coating of polymer thin-film transistors, *Nat. Commun.*, 2012, **3**(1), 1176.
74 J. A. Rogers, Z. Bao, A. Makhija and P. Braun, Printing Process Suitable for Reel-to-Reel Production of High-Performance Organic Transistors and Circuits, *Adv. Mater.*, 1999, **11**(9), 741–745.
75 U. Zschieschang, H. Klauk, M. Halik, G. Schmid and C. Dehm, Flexible Organic Circuits with Printed Gate Electrodes, *Adv. Mater.*, 2003, **15**(14), 1147–1151.

76 T. Cao, Q. Xu, A. Winkleman and G. M. Whitesides, Fabrication of Thin, Metallic Films along the Sidewalls of a Topographically Patterned Stamp and Their Application in Charge Printing, *Small*, 2005, **1**(12), 1191–1195.
77 P. Costa, J. E. Gautrot and J. T. Connelly, Directing cell migration using micropatterned and dynamically adhesive polymer brushes, *Acta Biomater.*, 2014, **10**(6), 2415–2422.
78 L. Chen, C. Yan and Z. Zheng, Functional polymer surfaces for controlling cell behaviors, *Mater. Today*, 2018, **21**(1), 38–59.
79 R. D. Piner, J. Zhu, F. Xu, S. Hong and C. A. Mirkin, "Dip-Pen" Nanolithography, *Science*, 1999, **283**(5402), 661–663.
80 Y. B. Lee, S.-j. Kim, E. M. Kim, H. Byun, H.-k. Chang, J. Park, Y. S. Choi and H. Shin, Microcontact printing of polydopamine on thermally expandable hydrogels for controlled cell adhesion and delivery of geometrically defined microtissues, *Acta Biomater.*, 2017, **61**, 75–87.
81 Y. Li, B. W. Maynor and J. Liu, Electrochemical AFM "Dip-Pen" Nanolithography, *J. Am. Chem. Soc.*, 2001, **123**(9), 2105–2106.
82 B. A. Nelson, W. P. King, A. R. Laracuente, P. E. Sheehan and L. J. Whitman, Direct deposition of continuous metal nanostructures by thermal dip-pen nanolithography, *Appl. Phys. Lett.*, 2006, **88**(3), 033104.
83 D. A. Weinberger, S. Hong, C. A. Mirkin, B. W. Wessels and T. B. Higgins, Combinatorial Generation and Analysis of Nanometer- and Micrometer-Scale Silicon Features via "Dip-Pen" Nanolithography and Wet Chemical Etching, *Adv. Mater.*, 2000, **12**(21), 1600–1603.
84 H.-T. Wang, O. A. Nafday, J. R. Haaheim, E. Tevaarwerk, N. A. Amro, R. G. Sanedrin, C.-Y. Chang, F. Ren and S. J. Pearton, Toward conductive traces: Dip Pen Nanolithography® of silver nanoparticle-based inks, *Appl. Phys. Lett.*, 2008, **93**(14), 143105.
85 S.-C. Hung, O. A. Nafday, J. R. Haaheim, F. Ren, G. C. Chi and S. J. Pearton, Dip Pen Nanolithography of Conductive Silver Traces, *J. Phys. Chem. C*, 2010, **114**(21), 9672–9677.
86 A. Hernandez-Santana, E. Irvine, K. Faulds and D. Graham, Rapid prototyping of poly(dimethoxysiloxane) dot arrays by dip-pen nanolithography, *Chem. Sci.*, 2011, **2**(2), 211–215.
87 L. M. Demers, D. S. Ginger, S. J. Park, Z. Li, S. W. Chung and C. A. Mirkin, Direct patterning of modified oligonucleotides on metals and insulators by dip-pen nanolithography, *Science*, 2002, **296**(5574), 1836–1838.
88 S. W. Chung, D. S. Ginger, M. W. Morales, Z. Zhang, V. Chandrasekhar, M. A. Ratner and C. A. Mirkin, Top-down meets bottom-up: dip-pen nanolithography and DNA-directed assembly of nanoscale electrical circuits, *Small*, 2005, **1**(1), 64–69.
89 K.-B. Lee, J.-H. Lim and C. A. Mirkin, Protein Nanostructures Formed via Direct-Write Dip-Pen Nanolithography, *J. Am. Chem. Soc.*, 2003, **125**(19), 5588–5589.
90 J.-H. Lim, D. S. Ginger, K.-B. Lee, J. Heo, J.-M. Nam and C. A. Mirkin, Direct-Write Dip-Pen Nanolithography of Proteins on Modified Silicon Oxide Surfaces, *Angew. Chem., Int. Ed.*, 2003, **42**(20), 2309–2312.
91 K.-B. Lee, S.-J. Park, C. A. Mirkin, J. C. Smith and M. Mrksich, Protein Nanoarrays Generated By Dip-Pen Nanolithography, *Science*, 2002, **295**(5560), 1702–1705.
92 M. Lee, D.-K. Kang, H.-K. Yang, K.-H. Park, S. Y. Choe, C. Kang, S.-I. Chang, M. H. Han and I.-C. Kang, Protein nanoarray on Prolinker™ surface constructed by atomic force microscopy dip-pen nanolithography for analysis of protein interaction, *Proteomics*, 2006, **6**(4), 1094–1103.
93 E. J. Irvine, A. Hernandez-Santana, K. Faulds and D. Graham, Fabricating protein immunoassay arrays on nitrocellulose using dip-pen lithography techniques, *Analyst*, 2011, **136**(14), 2925–2930.
94 Y. Cho and A. Ivanisevic, TAT Peptide Immobilization on Gold Surfaces: A Comparison Study with a Thiolated Peptide and Alkylthiols Using AFM, XPS, and FT-IRRAS, *J. Phys. Chem. B*, 2005, **109**(13), 6225–6232.
95 Y. Cho and A. Ivanisevic, SiOx Surfaces with Lithographic Features Composed of a TAT Peptide, *J. Phys. Chem. B*, 2004, **108**(39), 15223–15228.
96 H. Jiang and S. I. Stupp, Dip-Pen Patterning and Surface Assembly of Peptide Amphiphiles, *Langmuir*, 2005, **21**(12), 5242–5246.
97 X. Liu, L. Fu, S. Hong, V. P. Dravid and C. A. Mirkin, Arrays of Magnetic Nanoparticles Patterned via "Dip-Pen" Nanolithography, *Adv. Mater.*, 2002, **14**(3), 231–234.
98 D. Roy, M. Munz, P. Colombi, S. Bhattacharyya, J.-P. Salvetat, P. J. Cumpson and M.-L. Saboungi, Directly writing with nanoparticles at the nanoscale using dip-pen nanolithography, *Appl. Surf. Sci.*, 2007, **254**(5), 1394–1398.
99 W. M. Wang, R. M. Stoltenberg, S. Liu and Z. Bao, Direct Patterning of Gold Nanoparticles Using Dip-Pen Nanolithography, *ACS Nano*, 2008, **2**(10), 2135–2142.
100 P. Xu, H. Uyama, J. E. Whitten, S. Kobayashi and D. L. Kaplan, Peroxidase-Catalyzed in Situ Polymerization of Surface Orientated Caffeic Acid, *J. Am. Chem. Soc.*, 2005, **127**(33), 11745–11753.
101 M. Yang, P. E. Sheehan, W. P. King and L. J. Whitman, Direct Writing of a Conducting Polymer with Molecular-Level Control of Physical Dimensions and Orientation, *J. Am. Chem. Soc.*, 2006, **128**(21), 6774–6775.
102 J.-H. Lim and C. A. Mirkin, Electrostatically Driven Dip-Pen Nanolithography of Conducting Polymers, *Adv. Mater.*, 2002, **14**(20), 1474–1477.
103 R. McKendry, W. T. S. Huck, B. Weeks, M. Fiorini, C. Abell and T. Rayment, Creating Nanoscale Patterns of Dendrimers on Silicon Surfaces with Dip-Pen Nanolithography, *Nano Lett.*, 2002, **2**(7), 713–716.
104 P. Xu and D. L. Kaplan, Horseradish Peroxidase Catalyzed Polymerization of Tyrosine Derivatives for Nanoscale Surface Patterning, *J. Macromol. Sci., Part A: Pure Appl. Chem.*, 2004, **41**(12), 1437–1445.
105 X. Liu, Y. Li and Z. Zheng, Programming nanostructures of polymer brushes by dip-pen nanodisplacement lithography (DNL), *Nanoscale*, 2010, **2**(12), 2614–2618.

106 R. Szoszkiewicz, T. Okada, S. C. Jones, T.-D. Li, W. P. King, S. R. Marder and E. Riedo, High-Speed, Sub-15 nm Feature Size Thermochemical Nanolithography, *Nano Lett.*, 2007, **7**(4), 1064–1069.

107 D. Wang, S. Kim, W. D. Underwood II, A. J. Giordano, C. L. Henderson, Z. Dai, W. P. King, S. R. Marder and E. Riedo, Direct writing and characterization of poly(p-phenylene vinylene) nanostructures, *Appl. Phys. Lett.*, 2009, **95**(23), 233108.

108 K. G. Sharp, G. S. Blackman, N. J. Glassmaker, A. Jagota and C.-Y. Hui, Effect of Stamp Deformation on the Quality of Microcontact Printing: Theory and Experiment, *Langmuir*, 2004, **20**(15), 6430–6438.

109 C. Y. Hui, A. Jagota, Y. Y. Lin and E. J. Kramer, Constraints on Microcontact Printing Imposed by Stamp Deformation, *Langmuir*, 2002, **18**(4), 1394–1407.

110 F. Huo, Z. Zheng, G. Zheng, L. R. Giam, H. Zhang and C. A. Mirkin, Polymer Pen Lithography, *Science*, 2008, **321**(5896), 1658–1660.

111 D. J. Eichelsdoerfer, X. Liao, M. D. Cabezas, W. Morris, B. Radha, K. A. Brown, L. R. Giam, A. B. Braunschweig and C. A. Mirkin, Large-area molecular patterning with polymer pen lithography, *Nat. Protoc.*, 2013, **8**(12), 2548–2560.

112 K. Salaita, Y. Wang, J. Fragala, R. A. Vega, C. Liu and C. A. Mirkin, Massively Parallel Dip–Pen Nanolithography with 55 000-Pen Two-Dimensional Arrays, *Angew. Chem., Int. Ed.*, 2006, **45**(43), 7220–7223.

113 E. Rani, S. A. Mohshim, M. Z. Ahmad, R. Goodacre, S. A. Alang Ahmad and L. S. Wong, Polymer Pen Lithography-Fabricated DNA Arrays for Highly Sensitive and Selective Detection of Unamplified Ganoderma Boninense DNA, *Polymers*, 2019, **11**(3), 561.

114 R. Kumar, S. Weigel, R. Meyer, C. M. Niemeyer, H. Fuchs and M. Hirtz, Multi-color polymer pen lithography for oligonucleotide arrays, *Chem. Commun.*, 2016, **52**(83), 12310–12313.

115 Z. Zheng, W. L. Daniel, L. R. Giam, F. Huo, A. J. Senesi, G. Zheng and C. A. Mirkin, Multiplexed Protein Arrays Enabled by Polymer Pen Lithography: Addressing the Inking Challenge, *Angew. Chem., Int. Ed.*, 2009, **48**(41), 7626–7629.

116 F. Brinkmann, M. Hirtz, A. M. Greiner, M. Weschenfelder, B. Waterkotte, M. Bastmeyer and H. Fuchs, Interdigitated Multicolored Bioink Micropatterns by Multiplexed Polymer Pen Lithography, *Small*, 2013, **9**(19), 3266–3275.

117 A. Angelin, U. Bog, R. Kumar, C. M. Niemeyer and M. Hirtz, Writing Behavior of Phospholipids in Polymer Pen Lithography (PPL) for Bioactive Micropatterns, *Polymers*, 2019, **11**(5), 891.

118 R. Kumar, A. Urtizberea, S. Ghosh, U. Bog, Q. Rainer, S. Lenhert, H. Fuchs and M. Hirtz, Polymer Pen Lithography with Lipids for Large-Area Gradient Patterns, *Langmuir*, 2017, **33**(35), 8739–8748.

119 S. Bian, J. He, K. B. Schesing and A. B. Braunschweig, Polymer Pen Lithography (PPL)-Induced Site-Specific Click Chemistry for the Formation of Functional Glycan Arrays, *Small*, 2012, **8**(13), 2000–2005.

120 S. Bian, K. B. Schesing and A. B. Braunschweig, Matrix-assisted polymer pen lithography induced Staudinger Ligation, *Chem. Commun.*, 2012, **48**(41), 4995–4997.

121 Z. Xie, C. Chen, X. Zhou, T. Gao, D. Liu, Q. Miao and Z. Zheng, Massively Parallel Patterning of Complex 2D and 3D Functional Polymer Brushes by Polymer Pen Lithography, *ACS Appl. Mater. Interfaces*, 2014, **6**(15), 11955–11964.

122 U. Bog, A. de los Santos Pereira, S. L. Mueller, S. Havenridge, V. Parrillo, M. Bruns, A. E. Holmes, C. Rodriguez-Emmenegger, H. Fuchs and M. Hirtz, Clickable Antifouling Polymer Brushes for Polymer Pen Lithography, *ACS Appl. Mater. Interfaces*, 2017, **9**(13), 12109–12117.

123 L. Huang, A. B. Braunschweig, W. Shim, L. Qin, J. K. Lim, S. J. Hurst, F. Huo, C. Xue, J.-W. Jang and C. A. Mirkin, Matrix-Assisted Dip-Pen Nanolithography (MA-DPN) and Polymer Pen Lithography (MA-PPL), *Small*, 2010, **6**(10), 1077–1081.

124 S. Biswas, F. Brinkmann, M. Hirtz and H. Fuchs, Patterning of Quantum Dots by Dip-Pen and Polymer Pen Nanolithography, *Nanofabrication*, 2015, **2**, 19–26.

125 J. S. Du, P.-C. Chen, B. Meckes, Z. Xie, J. Zhu, Y. Liu, V. P. Dravid and C. A. Mirkin, The Structural Fate of Individual Multicomponent Metal-Oxide Nanoparticles in Polymer Nanoreactors, *Angew. Chem., Int. Ed.*, 2017, **56**(26), 7625–7629.

126 G. Arrabito, H. Schroeder, K. Schroder, C. Filips, U. Marggraf, C. Dopp, M. Venkatachalapathy, L. Dehmelt, P. I. Bastiaens, A. Neyer and C. M. Niemeyer, Configurable low-cost plotter device for fabrication of multi-color sub-cellular scale microarrays, *Small*, 2014, **10**(14), 2870–2876.

127 F. Huo, G. Zheng, X. Liao, L. R. Giam, J. Chai, X. Chen, W. Shim and C. A. Mirkin, Beam pen lithography, *Nat. Nanotechnol.*, 2010, **5**(9), 637–640.

128 C. Carbonell, D. J. Valles, A. M. Wong, M. W. Tsui, M. Niang and A. B. Braunschweig, Massively Multiplexed Tip-Based Photochemical Lithography under Continuous Capillary Flow, *Chem*, 2018, **4**(4), 857–867.

129 Y. Zhou, Z. Xie, K. A. Brown, D. J. Park, X. Zhou, P.-C. Chen, M. Hirtz, Q.-Y. Lin, V. P. Dravid, G. C. Schatz, Z. Zheng and C. A. Mirkin, Apertureless Cantilever-Free Pen Arrays for Scanning Photochemical Printing, *Small*, 2015, **11**(8), 913–918.

130 S. Bian, S. B. Zieba, W. Morris, X. Han, D. C. Richter, K. A. Brown, C. A. Mirkin and A. B. Braunschweig, Beam pen lithography as a new tool for spatially controlled photochemistry, and its utilization in the synthesis of multivalent glycan arrays, *Chem. Sci.*, 2014, **5**(5), 2023–2030.

131 S. He, Z. Xie, D. J. Park, X. Liao, K. A. Brown, P.-C. Chen, Y. Zhou, G. C. Schatz and C. A. Mirkin, Liquid-Phase Beam Pen Lithography, *Small*, 2016, **12**(8), 988–993.

132 Z. Huang, L. R. Powell, X. Wu, M. Kim, H. Qu, P. Wang, J. L. Fortner, B. Xu, A. L. Ng and Y. Wang, Photolithographic Patterning of Organic Color-Centers, *Adv. Mater.*, 2020, **32**(14), 1906517.

133 Z. Xie, Y. Zhou, J. L. Hedrick, P.-C. Chen, S. He, M. M. Shahjamali, S. Wang, Z. Zheng and C. A. Mirkin, On-Tip Photo-Modulated Molecular Printing, *Angew. Chem., Int. Ed.*, 2015, **54**(44), 12894–12899.

134 Z. Xie, P. Gordiichuk, Q.-Y. Lin, B. Meckes, P.-C. Chen, L. Sun, J. S. Du, J. Zhu, Y. Liu, V. P. Dravid and C. A. Mirkin, Solution-Phase Photochemical Nanopatterning Enabled by High-Refractive-Index Beam Pen Arrays, *ACS Nano*, 2017, **11**(8), 8231–8241.

135 Z. Huang, L. Li, X. A. Zhang, N. Alsharif, X. Wu, Z. Peng, X. Cheng, P. Wang, K. A. Brown and Y. Wang, Photoactuated Pens for Molecular Printing, *Adv. Mater.*, 2018, **30**(8), 1705303.

136 J. Zhu, H. Lin, Y. Kim, M. Yang, K. Skakuj, J. S. Du, B. Lee, G. C. Schatz, R. P. Van Duyne and C. A. Mirkin, Light-Responsive Colloidal Crystals Engineered with DNA, *Adv. Mater.*, 2020, **32**(8), 1906600.

137 X. M. Liu, C. Carbonell and A. B. Braunschweig, Towards Scanning Probe Lithography-Based 4D Nanoprinting by Advancing Surface Chemistry, Nanopatterning Strategies, and Characterization Protocols, *Chem. Soc. Rev.*, 2016, **45**(22), 6289–6310.

138 W. T. Müller, D. L. Klein, T. Lee, J. Clarke, P. L. McEuen and P. G. Schultz, A strategy for the chemical synthesis of nanostructures, *Science*, 1995, **268**(5208), 272–273.

139 S. Takeda, C. Nakamura, C. Miyamoto, N. Nakamura, M. Kageshima, H. Tokumoto and J. Miyake, Lithographing of Biomolecules on a Substrate Surface Using an Enzyme-Immobilized AFM Tip, *Nano Lett.*, 2003, **3**(11), 1471–1474.

140 A. B. Braunschweig, A. J. Senesi and C. A. Mirkin, Redox-Activating Dip-Pen Nanolithography (RA-DPN), *J. Am. Chem. Soc.*, 2009, **131**, 922–923.

141 S. Bian, A. M. Scott, Y. Cao, Y. Liang, S. Osuna, K. N. Houk and A. B. Braunschweig, Covalently Patterned Graphene Surfaces by a Force Accelerated Diels-Alder Reaction, *J. Am. Chem. Soc.*, 2013, **134**, 9240–9243.

142 X. Liu, Y. Zheng, S. R. Peurifoy, E. A. Kothari and A. B. Braunschweig, Optimization of 4D polymer printing within a massively parallel flow-through photochemical microreactor, *Polym. Chem.*, 2016, **7**(19), 3229–3235.

143 A. M. Wong, D. J. Valles, C. Carbonell, C. L. Chambers, A. Y. Rozenfeld, R. W. Aldasooky and A. B. Braunschweig, Controlled-Height Brush Polymer Patterns via Surface-Initiated Thiol-Methacrylate Photopolymerizations, *ACS Macro Lett.*, 2019, **8**(11), 1474–1478.

144 H. C. Kolb, M. G. Finn and K. B. Sharpless, Click Chemistry: Diverse Chemical Function from a Few Good Reactions, *Angew. Chem., Int. Ed.*, 2001, **40**(11), 2004–2021.

145 S. D. Bian, K. B. Schesing and A. B. Braunschweig, Matrix-assisted polymer pen lithography induced Staudinger Ligation, *Chem. Commun.*, 2012, **48**(41), 4995–4997.

146 N. B. Cramer and C. N. Bowman, Kinetics of thiol–ene and thiol–acrylate photopolymerizations with real-time fourier transform infrared, *J. Polym. Sci., Part A: Polym. Chem.*, 2001, **39**(19), 3311–3319.

147 C. E. Hoyle and C. N. Bowman, Thiol–Ene Click Chemistry, *Angew. Chem., Int. Ed.*, 2010, **49**(9), 1540–1573.

148 C. E. Hoyle, A. B. Lowe and C. N. Bowman, Thiol-click chemistry: a multifaceted toolbox for small molecule and polymer synthesis, *Chem. Soc. Rev.*, 2010, **39**(4), 1355–1387.

149 G. Arrabito, H. Schroeder, K. Schröder, C. Filips, U. Marggraf, C. Dopp, M. Venkatachalapathy, L. Dehmelt, P. I. H. Bastiaens, A. Neyer and C. M. Niemeyer, Configurable Low-Cost Plotter Device for Fabrication of Multi-Color Sub-Cellular Scale Microarrays, *Small*, 2014, **10**(14), 2870–2876.

150 S. M. Dimick, S. C. Powell, S. A. McMahon, D. N. Moothoo, J. H. Naismith and E. J. Toone, On the Meaning of Affinity: Cluster Glycoside Effects and Concanavalin A, *J. Am. Chem. Soc.*, 1999, **121**(44), 10286–10296.

151 J. J. Lundquist and E. J. Toone, The cluster glycoside effect, *Chem. Rev.*, 2002, **102**(2), 555–578.

152 O. Blixt, S. Head, T. Mondala, C. Scanlan, M. E. Huflejt, R. Alvarez, M. C. Bryan, F. Fazio, D. Calarese, J. Stevens, N. Razi, D. J. Stevens, J. J. Skehel, I. van Die, D. R. Burton, I. A. Wilson, R. Cummings, N. Bovin, C.-H. Wong and J. C. Paulson, Printed covalent glycan array for ligand profiling of diverse glycan binding proteins, *Proc. Natl. Acad. U. S. A.*, 2004, **101**(49), 17033–17038.

153 O. Oyelaran and J. C. Gildersleeve, Glycan arrays: recent advances and future challenges, *Curr. Opin. Chem. Biol.*, 2009, **13**(4), 406–413.

154 L. L. Kiessling and R. A. Splain, Chemical Approaches to Glycobiology, *Annu. Rev. Biochem.*, 2010, **79**, 619–653.

155 G.-D. Syu, J. Dunn and H. Zhu, Developments and Applications of Functional Protein Microarrays, *Mol. Cell. Proteomics*, 2020, **19**(6), 916–927.

156 M. Mende, V. Bordoni, A. Tsouka, F. F. Loeffler, M. Delbianco and P. H. Seeberger, Multivalent glycan arrays, *Faraday Discuss.*, 2019, **219**(0), 9–32.

157 C. Gao, M. Wei, T. R. McKitrick, A. M. McQuillan, J. Heimburg-Molinaro and R. D. Cummings, Glycan Microarrays as Chemical Tools for Identifying Glycan Recognition by Immune Proteins, *Front. Chem.*, 2019, **7**, 833.

158 J. Y. Hyun, J. Pai and I. Shin, The Glycan Microarray Story from Construction to Applications, *Acc. Chem. Res.*, 2017, **50**(4), 1069–1078.

159 S. Park, J. C. Gildersleeve, O. Blixt and I. Shin, Carbohydrate microarrays, *Chem. Soc. Rev.*, 2013, **42**(10), 4310–4326.

160 J. S. Temme, C. T. Campbell and J. C. Gildersleeve, Factors contributing to variability of glycan microarray binding profiles, *Faraday Discuss.*, 2019, **219**, 90–111.

161 A. E. Rydholm, C. N. Bowman and K. S. Anseth, Degradable thiol-acrylate photopolymers: polymerization and degradation behavior of an in situ forming biomaterial, *Biomaterials*, 2005, **26**(22), 4495–4506.

162 A. E. Rydholm, N. L. Held, D. S. W. Benoit, C. N. Bowman and K. S. Anseth, Modifying network chemistry in thiol-acrylate photopolymers through postpolymerization functionalization to control cell-material interactions, *J. Biomed. Mater. Res., Part A*, 2008, **86A**(1), 23–30.

163 A. E. Rydholm, S. K. Reddy, K. S. Anseth and C. N. Bowman, Controlling Network Structure in Degradable Thiol–Acrylate Biomaterials to Tune Mass Loss Behavior, *Biomacromolecules*, 2006, **7**(10), 2827–2836.

164 C. N. Salinas and K. S. Anseth, Mixed Mode Thiol–Acrylate Photopolymerizations for the Synthesis of PEG–Peptide Hydrogels, *Macromolecules*, 2008, **41**(16), 6019–6026.

165 A. Fu, K. Gwon, M. Kim, G. Tae and J. A. Kornfield, Visible-Light-Initiated Thiol–Acrylate Photopolymerization of Heparin-Based Hydrogels, *Biomacromolecules*, 2015, **16**(2), 497–506.

166 J. Choi, P. Schattling, F. D. Jochum, J. Pyun, K. Char and P. Theato, Functionalization and patterning of reactive polymer brushes based on surface reversible addition and fragmentation chain transfer polymerization, *J. Polym. Sci., Part A: Polym. Chem.*, 2012, **50**(19), 4010–4018.

167 A. Rastogi, M. Y. Paik, M. Tanaka and C. K. Ober, Direct Patterning of Intrinsically Electron Beam Sensitive Polymer Brushes, *ACS Nano*, 2010, **4**(2), 771–780.

168 K. Matyjaszewski, Atom Transfer Radical Polymerization (ATRP): Current Status and Future Perspectives, *Macromolecules*, 2012, **45**(10), 4015–4039.

169 K. Matyjaszewski and J. Xia, Atom Transfer Radical Polymerization, *Chem. Rev.*, 2001, **101**(9), 2921–2990.

170 B. Narupai, Z. A. Page, N. J. Treat, A. J. McGrath, C. W. Pester, E. H. Discekici, N. D. Dolinski, G. F. Meyers, J. Read de Alaniz and C. J. Hawker, Simultaneous Preparation of Multiple Polymer Brushes under Ambient Conditions using Microliter Volumes, *Angew. Chem., Int. Ed.*, 2018, **57**(41), 13433–13438.

171 J.-S. Wang and K. Matyjaszewski, Controlled/"Living" Radical Polymerization. Halogen Atom Transfer Radical Polymerization Promoted by a Cu(I)/Cu(II) Redox Process, *Macromolecules*, 1995, **28**(23), 7901–7910.

172 Y. Li, J. Zhang, L. Fang, L. Jiang, W. Liu, T. Wang, L. Cui, H. Sun and B. Yang, Polymer brush nanopatterns with controllable features for protein pattern applications, *J. Mater. Chem.*, 2012, **22**(48), 25116–25122.

173 G. Panzarasa, G. Soliveri, K. Sparnacci and S. Ardizzone, Patterning of polymer brushes made easy using titanium dioxide: direct and remote photocatalytic lithography, *Chem. Commun.*, 2015, **51**(34), 7313–7316.

174 S. J. Ahn, M. Kaholek, W.-K. Lee, B. LaMattina, T. H. LaBean and S. Zauscher, Surface-Initiated Polymerization on Nanopatterns Fabricated by Electron-Beam Lithography, *Adv. Mater.*, 2004, **16**(23–24), 2141–2145.

175 L. Fu, Z. Wang, S. Lathwal, A. E. Enciso, A. Simakova, S. R. Das, A. J. Russell and K. Matyjaszewski, Synthesis of Polymer Bioconjugates via Photoinduced Atom Transfer Radical Polymerization under Blue Light Irradiation, *ACS Macro Lett.*, 2018, **7**(10), 1248–1253.

176 F. Zhou, Z. Zheng, B. Yu, W. Liu and W. T. S. Huck, Multicomponent Polymer Brushes, *J. Am. Chem. Soc.*, 2006, **128**(50), 16253–16258.

177 K. B. Buhl, A. H. Agergaard, M. Lillethorup, J. P. Nikolajsen, S. U. Pedersen and K. Daasbjerg, Polymer Brush Coating and Adhesion Technology at Scale, *Polymers*, 2020, **12**(7), 1475.

178 D. Li, L. Xu, J. Wang and J. E. Gautrot, Responsive Polymer Brush Design and Emerging Applications for Nanotheranostics, *Adv. Healthcare Mater.*, 2021, **10**(5), 2000953.

179 I. Luzinov, S. Minko and V. V. Tsukruk, Adaptive and responsive surfaces through controlled reorganization of interfacial polymer layers, *Prog. Polym. Sci.*, 2004, **29**(7), 635–698.

180 M. A. C. Stuart, W. T. S. Huck, J. Genzer, M. Müller, C. Ober, M. Stamm, G. B. Sukhorukov, I. Szleifer, V. V. Tsukruk, M. Urban, F. Winnik, S. Zauscher, I. Luzinov and S. Minko, Emerging applications of stimuli-responsive polymer materials, *Nat. Mater.*, 2010, **9**(2), 101–113.

181 D. C. Leslie, A. Waterhouse, J. B. Berthet, T. M. Valentin, A. L. Watters, A. Jain, P. Kim, B. D. Hatton, A. Nedder, K. Donovan, E. H. Super, C. Howell, C. P. Johnson, T. L. Vu, D. E. Bolgen, S. Rifai, A. R. Hansen, M. Aizenberg, M. Super, J. Aizenberg and D. E. Ingber, A bioinspired omniphobic surface coating on medical devices prevents thrombosis and biofouling, *Nat. Biotechnol.*, 2014, **32**(11), 1134–1140.

182 L. Chen, Z. Xie, T. Gan, Y. Wang, G. Zhang, C. A. Mirkin and Z. Zheng, Biomimicking Nano-Micro Binary Polymer Brushes for Smart Cell Orientation and Adhesion Control, *Small*, 2016, **12**(25), 3400–3406.

183 Essentials of Glycobiology, in *Essentials of Glycobiology*, ed. A. Varki, R. D. Cummings, J. D. Esko, H. H. Freeze, P. Stanley, C. R. Bertozzi, G. W. Hart and M. E. Etzler, Cold Spring Harbor Laboratory Press, Copyright © 2009, The Consortium of Glycobiology Editors, La Jolla, California, Cold Spring Harbor (NY), 2009.

184 M. E. Welch and C. K. Ober, Responsive and patterned polymer brushes, *J. Polym. Sci., Part B: Polym. Phys.*, 2013, **51**(20), 1457–1472.

185 T. Chen, I. Amin and R. Jordan, Patterned polymer brushes, *Chem. Soc. Rev.*, 2012, **41**(8), 3280–3296.

186 M. Kim, S. K. Schmitt, J. W. Choi, J. D. Krutty and P. Gopalan, From Self-Assembled Monolayers to Coatings: Advances in the Synthesis and Nanobio Applications of Polymer Brushes, *Polymers*, 2015, **7**(7), 1346–1378.

187 T. Wu, P. Gong, I. Szleifer, P. Vlček, V. Šubr and J. Genzer, Behavior of Surface-Anchored Poly(acrylic acid) Brushes

with Grafting Density Gradients on Solid Substrates: 1. Experiment, *Macromolecules*, 2007, **40**(24), 8756–8764.

188 B. P. Harris and A. T. Metters, Generation and Characterization of Photopolymerized Polymer Brush Gradients, *Macromolecules*, 2006, **39**(8), 2764–2772.

189 M. Rafti, J. A. Allegretto, G. M. Segovia, J. S. Tuninetti, J. M. Giussi, E. Bindini and O. Azzaroni, Metal–organic frameworks meet polymer brushes: enhanced crystalline film growth induced by macromolecular primers, *Mater. Chem. Front.*, 2017, **1**(11), 2256–2260.

190 T. Kamada, Y. Yamazawa, T. Nakaji-Hirabayashi, H. Kitano, Y. Usui, Y. Hiroi and T. Kishioka, Patterning of photocleavable zwitterionic polymer brush fabricated on silicon wafer, *Colloids Surf., B*, 2014, **123**, 878–886.

191 K. Kuroda, H. Miyoshi, S. Fujii, T. Hirai, A. Takahara, A. Nakao, Y. Iwasaki, K. Morigaki, K. Ishihara and S.-i. Yusa, Poly(dimethylsiloxane) (PDMS) surface patterning by biocompatible photo-crosslinking block copolymers, *RSC Adv.*, 2015, **5**(58), 46686–46693.

192 H. L. Huang, J.-K. Chen and M. P. Houng, Fabrication of two-dimensional periodic relief grating of tethered polystyrene on silicon surface as solvent sensors, *Sens. Actuators, B*, 2013, **177**, 833–840.

193 A. Sangsuwan, B. Narupai, P. Sae-ung, S. Rodtamai, N. Rodthongkum and V. P. Hoven, Patterned Poly(acrylic acid) Brushes Containing Gold Nanoparticles for Peptide Detection by Surface-Assisted Laser Desorption/Ionization Mass Spectrometry, *Anal. Chem.*, 2015, **87**(21), 10738–10746.

194 Y. Xu, M. Shinomiya and A. Harada, Soft Matter-Regulated Active Nanovalves Locally Self-Assembled in Femtoliter Nanofluidic Channels, *Adv. Mater.*, 2016, **28**(11), 2209–2216.

195 T. Steentjes, S. Sarkar, P. Jonkheijm, S. G. Lemay and J. Huskens, Electron Transfer Mediated by Surface-Tethered Redox Groups in Nanofluidic Devices, *Small*, 2017, **13**(8), 1603268.

196 J.-K. Chen, J.-H. Wang, S.-K. Fan and J.-Y. Chang, Reversible Hydrophobic/Hydrophilic Adhesive of PS-b-PNIPAAm Copolymer Brush Nanopillar Arrays for Mimicking the Climbing Aptitude of Geckos, *J. Phys. Chem. C*, 2012, **116**(12), 6980–6992.

